EXPERIMENTAL STUDIES IN MATTER-WAVE LASERS

Efstathios Lambropoulos

Submitted in partial fulfillment of the requirements for the degree of Master of Science

Supervisors:

Wolf von Klitzing

Peter Rakitzis

Physics Department

University of Crete

IESL-FORTH

March 2017

Acknowledgments

This thesis was conducted in the Cretan Matter Waves laboratory, at the Institute of Electronic Structure and Laser (I.E.S.L. – FO.R.T.H.) under the supervision of the group leader Dr. Wolf von Klitzing, who I want to thank for both his guidance and his patience.

I would also like to thank my first lab colleagues, Hector Mas, Saurabh Pandey and Kostas Poulios for their help and support in and out of the lab as well as the lab colleagues I worked with later, Giannis Drougakis, Vasiliki Bolpasi, Kostas Mavrakis and Ivan Alonso Miguel.

Contents

Chapter 1 Introduction 3
Chapter 2 BEC 1 experimental setup 4
Overview of the experimental techniques for a BEC experiment 4
Susceptibility of the experiment to temperature fluctuations 7
Chapter 3 Control Theory 8
A basic introduction 8
Mathematical description 9
State-space models 9
Definition of the control problem 10
Dynamics under the influence of an input 10
Modeling the plant: Linear Time Invariant systems 11
Impulse response 12
Important system properties 12
The frequency domain approach 14
Transfer functions 15
Feedback 17
Types of feedback control 18
Tuning methods 19
Chapter 4 Stabilizing the temperature on the experiment 21
Position of the problem 21
Overview of the new stabilization system 30
Principle of operation 32
Chapter 5 The effect of the temperature stabilization on the cold atoms 38
Chapter 6 Summary and conclusions 44
Bibliography 45

Chapter 1 Introduction

In 1924 the existence of a new state of matter was theoretically predicted by Einstein and Bose, a state where the quantum nature of matter becomes macroscopically visible. More specifically, it was predicted that below a certain temperature, a phase transition occurs and a macroscopic number of bosons will occupy the lowest energy single particle state. This collective state was named Bose-Einstein condensate and was realized experimentally 71 years later, in 1995, by Ketterle and Wieman & Cornell, who were awarded with the Nobel Prize in Physics in 2001. An important aspect of laboratory requirements for the creation of Bose-Einstein condensates, is the thermal stability of the environment of the various stages of the experimental setup.

Normal air-conditioned laboratories provide a temperature stability of around ± 0.5°K (Dedman 2015). However, for Bose-Einstein condensation experiments, higher stability of the ambient temperature inside the experiment is critical for smooth operation and clean results. Optical components are susceptible to changes in the conditions of the surrounding environment. More specifically, optical fibers show fluctuations in the transmitted power, which depend on the ambient temperature fluctuations (Dvorak, 2014). Because the optical fibers are used in various stages of the experiment, and more specifically, provide the laser light for the magneto-optical trap (MOT), the fluctuations in transmitted power have a direct effect on both the position of the atomic cloud and the number of atoms that are trapped in the MOT. Furthermore, a reduction in the ambient temperature variations reduces the number of measurements one has to perform for a given quantity. Thus a system for high stability control of the temperature inside the experiment is essential.

Chapter 2 BEC 1 experimental setup

Overview of the experimental techniques for a BEC experiment

A variety of experimental techniques and hardware components are utilized for the realization of a Bose-Einstein condensate. High stability lasers, magnetic quadrupole traps and magneto-optical traps are used to cool and contain the rubidium atoms which make up the Bose-Einstein condensate. In this chapter, a brief overview of the techniques which are used is given. Since the temperature fluctuations affect the polarization-maintaining (PM) fibers, which are a key component, providing the laser light for magneto-optical trapping (as well as for cooling), the focus is going to be on the magneto-optical trap (MOT). Also, a brief discussion of the rest of the techniques and hardware that are used in the experiment is provided.

Magneto-Optical Trap (MOT)

The magneto-optical trap uses the magnetic field of a pair of circular coils and the light of opposing laser beams in order to contain the rubidium atoms used for the Bose-Einstein condensate. The two coils, with currents flowing in opposite directions, create a quadrupole field which is proportional to the distance from the origin and consequently is zero there (C.J. Pethick, 2008). Atoms experience a force proportional to the magnitude of the magnetic field and to the value of the M_J hyperfine sublevel number, which can take values from $-J$ to J. Therefore, atoms with positive M_J are moved away from the origin, whereas atoms with negative M_J move towards the origin. The magnetic field alone is not sufficient for confinement of the atoms, so pairs of counter-propagating laser beams are added. The laser frequency is slightly red-detuned from the atomic resonance frequency between the Zeeman levels caused by the magnetic field and the beam is circularly polarized. Due to the dependence of the magnitude of the energy split from the distance z ($\Delta E = -\boldsymbol{\mu B}$ with $|B| \sim z$), an atom with $M_J = -1$ moving away from the origin to $z > 0$, moves closer to resonance with the incoming laser light. Due to selection rules, a transition between Zeeman levels occurs only if $\Delta M_J = 0, \pm 1$, therefore atoms will absorb photons from the σ^- beam and will be forced to move back towards the origin. The opposite happens for atoms with $M_J = +1$ moving towards $z < 0$ which will absorb photons from the σ^+ beam and again will be forced to move towards the center of the trap. Depending on the number of counter-propagating beam pairs that are used (2 or 3) there can be confinement on a plane (2D MOT) or in space (3D MOT) (Bolpasi 2008).

Optical Molasses

Before being transferred to the magneto-optical trap, the atoms must be cooled down to a temperature in order to reduce their kinetic energy to the point where they cannot escape from the trap. This is achieved by applying the optical molasses technique, slowing the atoms down using laser light. Since the photons carry momentum, an atom absorbing a photon will experience a change in momentum. If an atom absorbs a photon with opposite momentum to that of its motion, it loses momentum, and, on average, it reemits the absorbed photons on all directions. After the atom has scattered many photons, there is an average deceleration of the atom, in the direction of the beam. Thus the atom experiences an average force opposite to its direction of motion, which is called a scattering force. In order to decelerate the atoms in all three directions, six counter-propagating beams are used. A stationary atom does not feel a force. However a moving atom will absorb photons due to the Doppler effect and will see the beams opposite to its movement as blue shifted and the counter-propagating beam red shifted. If the beams have a frequency below the atomic resonance frequency, the Doppler shift will bring the beams opposite to the atom's velocity closer to its resonance frequency, and thus the rate of absorption from that beam will be higher. This means that the atom will experience a greater force from a beam opposite to its motion, than from one parallel to its motion, decelerating in the process (Lett, 1989).

Re-pumping

The optical molasses beam in our case is detuned compared to the $F = 2 \rightarrow F' = 3$ transition in the D2 line of ^{87}Rb, therefore the cooling is done by transitions between these two states. There is a probability that atoms decay from the excited $F = 2$ state to the $F = 1$ state, which is unsuitable for the optical molasses technique, because of its distance from resonance with the optical molasses laser beams (6.8 GHz) (Bolpasi, 2008). For this reason, another laser beam is used to put the decaying atoms back into the $F = 2$ level, where they can absorb and emit light in order to be cooled down.

Optical pumping

The cooling provided by the optical molasses technique is not sufficient for the creation of a BEC. The atoms need to be transferred to the magneto-optical trap to be further cooled down. Because not all hyperfine states are suitable for trapping in a magnetic field, the optical pumping technique is used to prepare the atoms in the desired state. Atoms with $m_F > 0$ will move towards regions of lower magnetic field ("low-field seekers") while for $m_F < 0$ they will move towards high field regions ("high-field seekers"). Atoms with $m_F = 0$ are not affected by the magnetic field. Since the magnetic field of the MOT increases with distance, the atoms suitable for confinement are those with $m_F > 0$. To prepare the atoms in this state an optical pumping laser beam resonant

with the $F = 2 \rightarrow F' = 2$ transition is used which is circularly polarized, so that only the σ^+ transitions take place. Atoms move to higher hyperfine sublevels by absorbing photons under the condition $\Delta m_F = 1$ and decay to lower sublevels by emitting photons under the condition $\Delta m_F = 0, \pm 1$. The optical pumping beam excites the atoms to consecutively higher sublevels up to $m_F = +2$ state, while some of them decay back to lower sublevels. However, after a few transitions, all atoms end up on the $m_F = +2$ state where they cannot absorb any more photons and be further excited (C.J. Pethick, 2008), (Bolpasi, 2008).

Imaging of the BEC

After creating a BEC, information about its properties can be revealed by observing it. For that reason, an imaging technique must be introduced in order to image and then study the atoms contained in a BEC. For the imaging we use a laser beam resonant with the $F = 2 \rightarrow F' = 3$ transition. The imaging technique is based on the absorption of the imaging beam by the atoms. As the imaging beam is in resonance with the atoms, the atoms absorb some of the light of the beam, and the image that we get is essentially the shadow of the cloud. The image is taken by a high resolution CCD camera. According to this technique, two photographs must be taken, one without the atoms, and one with the atoms, so that we can subtract the one image from the other in order to eliminate the background light (Bolpasi, 2008).

Laser system

As discussed above, lasers are used in every step of a BEC experiment. The complexity of the experiment requires from the lasers a narrow linewidth (below 1MHz), tunable frequency, an ability to stabilize the frequency and sufficient optical power. Fluctuations in laser frequency have to be small compared to the linewidth $\Gamma/2\pi$ of the atomic transition that is of interest to us, which in this case is 6MHz. The total power needed must be approximately 600mW and it is such because the intensity of the laser must be higher than the saturation intensity I_s of the atoms, in our case, $I_s = 1.6 mW/cm^2$ (for circularly polarized light) (M. Pappa, 2011).

Diode lasers at 780nm are used for the experiment whose frequency is locked to the D2 line in ^{87}Rb by Doppler-free spectroscopy. The laser light is then used for injection-locking a diode which supplies us with the required intensity for the next stages at the same frequency as the laser used for injection. One diode is used with an external cavity and is called the "master laser" because its frequency and linewidth are forced onto the second diode which for this reason is called the slave laser. The slave laser has a microwave modulation of 6.6 GHz giving a main frequency and small sidebands. Light is then moved to an Acousto-Optic Modulation (AOM) board for small frequency shifts and

controlling of the amplitude for optical pumping, imaging and trapping (cooling and re-pumping). An optical fiber then guides the trapping laser light to an amplification system. The final beams are guided to the experiment through optical fibers.

Susceptibility of the experiment to temperature fluctuations

As shown in the previous sections, the experimental setup has many parts and some of them can be quite affected by temperature changes and not work optimally, therefore making the whole experiment less effective. Here are presented the major factors that contribute to the destabilization of the experimental setup.

Mechanical drifts

The experimental setup has a lot of optical components, such as mirrors, prisms, polarizing beam-splitters etc. that are supported by metallic mounts. Repeated expansion and contraction, due to thermal fluctuations, will cause these mounts to slowly drift out of their optimal position (Wilson, 2005), which in turn will lead to misalignment of said optical components and reduce the overall performance efficiency of the experiment. The most important sources of thermal fluctuations are due to changes in room temperature and heating of the optical components by the laser beams.

Polarization problems

As mentioned previously, the efficiency of optical fibers can be greatly affected by variations in ambient temperature. Namely, temperature fluctuations induce phase shifts in the polarization of the output beam, compared to that of the input beam (Zhang, 1993), on account of the dependence of the refractive indices of the fiber materials, on temperature. Any change in the polarization can have a considerable effect not only on the atom number, but also on the temperature, and even common-mode velocity of the atomic cloud.

Chapter 3 Control Theory

In this chapter a brief introduction on control theory is presented, with a focus on feedback control and the various tuning techniques, such as the Ziegler-Nichols methods that were used for tuning the stabilization system. This is done for reasons of completeness, as in most cases, it is not necessary to have a full mathematical description of a control problem and a heuristic approach is sufficient to have the desired level of control.

A basic introduction

Control theory is the cross-over branch of mathematics and engineering, which deals with the behavior of dynamical systems with inputs, and how their behavior changes by introducing feedback. Control theory is crucial for the design of high-precision devices which are used in a wide range of fields and applications, from industry to scientific laboratories.

Feedback control theory deals with the study of feedback control systems, meaning systems that use, discrete or continuous, measurements of the system output $y(t)$, in order to adjust the control input in real time (Geremia 2003). The output signal $y(t)$, is constantly being monitored and compared to a reference signal $r(t)$. The difference $r(t) - y(t)$ is known as the error signal $e(t)$. The aim of feedback controllers is to minimize the error signal's norm by generating a control signal $u^o(t)$.

Control theory aims to describe and design feedback control systems that satisfy the key properties of feedback control: performance, stability and robustness (Geremia 2003, 7).

- Performance, of a control system, is related to its capability to meet its control objectives (such as keeping the error signal small) successfully (John Doyle 1990, 3).
- Stability, is a measure of the control system's behavior, and is related to its response to external disturbances. A strict definition of stability is the system's ability to produce a bounded output for every bounded input. (Joseph DiStefano 1990, 114)
- Robustness, is the control system's ability to maintain a satisfying performance, in spite of changes in system being controlled or its environment (Astrom 2008, 17).

Depending on the application it is intended for, a real controller will a have balanced combination of the above three properties.

A typical feedback control system consists of four subsystems: a process to be controlled, sets of sensors and actuators, and a controller like in Figure 1 (Ozbay 1999, 2)

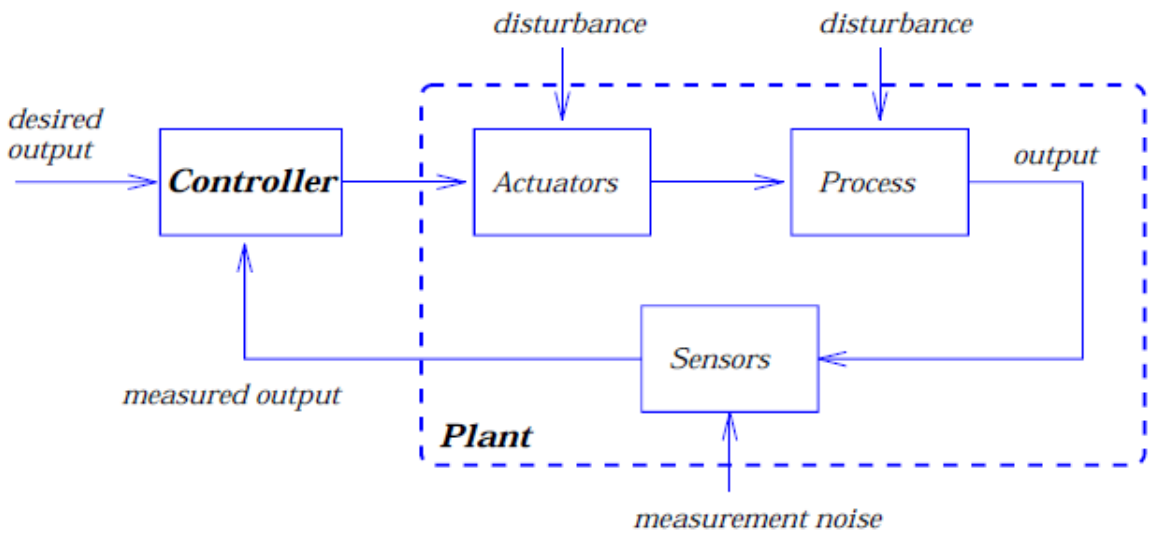

Figure 1:Typical feedback system.

The controller's job is to control the physical system that is called "process" in this context. However, when designing the controller, the influence of both the sensors and actuators present around or in the process have to be taken into account. The collective system of the process, the actuators and the sensors is called "the plant".

Mathematical description

State-space models

The state of a physical system can be described by a set of time-dependent variables, $\{x_1(t), x_2(t), \dots, x_n(t)\}$, $x_i(t) \in \mathbb{R}^n$, which form a vector , $\boldsymbol{x}(t)$. The state vector $\boldsymbol{x}(t)$ holds all the information about the system's past. The derivative of $\boldsymbol{x}(t)$ with respect to time $\frac{d}{dt}\boldsymbol{x}(t)$ gives us the time evolution of the state of the system and thus, the system can be represented by a differential equation (Astrom 2008, 31):

$$\frac{d}{dt}\boldsymbol{x}(t) = \boldsymbol{a}(\boldsymbol{x}, t), \text{ for } t \geq 0, \quad \text{Eq.1.1}$$

Where $\boldsymbol{a}(\boldsymbol{x}, t)$ is a state vector, is called the output function and represents the state of the system in a future time and thus contains all the information about the dynamics of it. The output function is both a function of time and the initial state vector. Since $\boldsymbol{a}(\boldsymbol{x}, t)$ depends on $\boldsymbol{x}(t)$ the dimension of the two vectors must be the same, i.e $a_i(t) \in \mathbb{R}^n$. Under real conditions, the information available about a physical system, is acquired by doing some sort of measurements onto the system. These measurements do not necessarily provide full information about the system, but only information that is of

interest to us. Therefore, an output function $\boldsymbol{y}(t) = \boldsymbol{c}(\boldsymbol{x}(t), t)$ (Astrom 2008, 31) resulting from a measurement, does not have to be of the same dimension as the initial state vector, i.e. if $x_i(t) \in \mathbb{R}^n$ then $y_i(t) \in \mathbb{R}^m$ with $n \neq m$. Figure 2 illustrates the concept of modeling the system's dynamics with a differential equation. So finally, a system can be represented by:

$$\frac{d}{dt}\boldsymbol{x}(t) = \boldsymbol{a}(\boldsymbol{x}, t), Eq.\ 1.1$$

$$\boldsymbol{y}(t) = \boldsymbol{c}(\boldsymbol{x}(t), t), Eq.\ 1.2$$

Definition of the control problem

If a term $\boldsymbol{u}(t) = \{u_1(t), u_2(t), \dots\}$ is introduced into Equation 1.1, the differential equation that appears, will generally have a different solution compared to that of 1.1, because of the dependence of $\boldsymbol{u}$ from time. In fact, such a term allows us to affect the time evolution of our system in a way that it meets a certain objective. Commonly, such an objective is keeping the system's output near a desired value called the reference signal $\boldsymbol{r}(t)$. The difference of the output signal and the reference signal is called the error signal, $\boldsymbol{e}(t) = \boldsymbol{r}(t) - \boldsymbol{y}(t)$ and finding an appropriate $\boldsymbol{u}$ signal that minimizes the norm of $\boldsymbol{e}$, $\|\boldsymbol{y}(t) - \boldsymbol{r}(t)\|$, is the problem that control theory deals with (Geremia 2003, 6).

Dynamics under the influence of an input

The mathematical analysis above describes the evolution of the system without any forces applied to it. By applying an input signal $(t) = \{u_1(t), \dots, u_k(t)\}$, $u_k \in \mathbb{R}^k$, the dynamics of the system can be manipulated(Astrom 2008, 31). The set of $u_k(t)$ are known as the control variables. In this case Eq.1.1 are modified into:

$$\frac{d}{dt}\boldsymbol{x}(t) = \boldsymbol{a}(\boldsymbol{x}, t) + \boldsymbol{b}(\boldsymbol{x}, \boldsymbol{u}),\ \text{Eq. 2.1}$$

$$\boldsymbol{y}(t) = \boldsymbol{c}(\boldsymbol{x}(t), \boldsymbol{u}(t), t)\ , \text{Eq. 2.2}$$

The function $\boldsymbol{b}(\boldsymbol{x}, \boldsymbol{u})$ contains the information about the interaction of the system in question with the applied input signal, so it is a function of both the initial state of the system, as well as the input signal. The input signal can have a different dimension from the state vector, but the function $\boldsymbol{b}(\boldsymbol{x}, \boldsymbol{u})$ has to be of the same dimension for mathematical consistency (Geremia 2003, 4). The concept is illustrated in Figure 2 below.

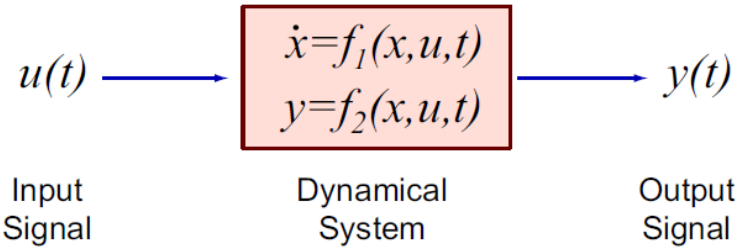

Figure 2: Modeling of a dynamical system :An input signal u(t) is applied to a dynamical system. The system's time evolution is determined by a function f_1 of the initial state x, the input signal and time. The output of the system is then projected into a function y(t).

Modeling the plant: Linear Time Invariant systems

Processes in feedback control theory are modeled as linear time-invariant systems. These systems satisfy the following conditions:

- *Linearity* means that the relationship between the input and the output of the system is a linear map: If input $x_1(t)$ produces response $y_1(t)$ and input $x_2(t)$ produces response $y_2(t)$ then the scaled and summed input $a_1x_1(t) + a_2x_2(t)$ produces the scaled and summed response $a_1y_1(t) + a_2y_2(t)$ where a_1 and a_2 are real or complex scalars. It follows that this can be extended to an arbitrary number of terms, and so for real numbers $c_1, c_2, c_3 \ldots, c_k$, input $\sum_k c_k x_k(t)$, produces the output $\sum_k c_k y_k(t)$. In particular, input $\int_{-\infty}^{+\infty} c_\omega x_\omega(t)\, d\omega$, produces output $\int_{-\infty}^{+\infty} c_\omega y_\omega(t)\, d\omega$, where $c_\omega$and x_ω are scalars and inputs that vary over a continuum indexed by ω. Thus if an input function can be represented by a continuum of input functions, combined "linearly", as shown, then the corresponding output function can be represented by the corresponding continuum of output functions, scaled and summed in the same way (Schetzen 2003, 34).
- *Time invariance* means that the relationship between the system's input and output does not change over time. That is, if input $x(t)$ produces an output $y(t)$ through an operation f, i.e. $y(t) = f(x(t))$ then time invariance implies $y(t + T) = f(x(t + T))$ for any time interval T. (Schetzen 2003, 5)

If we have an input that is a linear combination of waveforms such as $x(t) = \sum_k c_k v_k(t)$, then, because of the linearity of the system, the output is $y(t) = \sum_k c_k w_k(t)$, where w_k is the response of the system to v_k. If $v_k(t) = v(t - t_k)$, meaning each input is a time translation of a more general input, then time variance implies that $w_k(t) = w(t - t_k)$, where $v(t)$ gives the output $w(t)$. This means our

initial input can be re-written as $x(t) = \sum_k c_k v(t - t_k)$ and the output as $y(t) = \sum_k c_k w(t - t_k)$. Therefore, if the response of the system to a particular input is known, then its response to any input that is a linear combination of time translated waveforms of the known input, can be determined (Schetzen 2003, 37-38). This is a fundamental property of LTI systems.

Impulse response

The main result of LTI system theory is that a LTI system can be characterized entirely by a single function called the system's impulse response (Alan V. Oppenheim, 1996 p. 103). It can be shown (Schetzen 2003, 41-43) that by approximating the waveform of an input by a sum of rectangles of width ε and height $x(\varepsilon)$, x_ε, then the input can be written $x(t) = \lim_{\varepsilon \to 0} x_\varepsilon(t)$ and since linearity holds, the response of the system to x_ε is y_ε and the full response can be obtained $y(t) = \lim_{\varepsilon \to 0} y_\varepsilon(t)$. By utilizing the function $\delta_\varepsilon(t) = \begin{cases} \frac{1}{\varepsilon}, -\frac{\varepsilon}{2} \le t \le \frac{\varepsilon}{2} \\ 0 \; for \; all \; other \; t \end{cases}$, x_ε can be written as $x_\varepsilon(t) = \sum_{n\varepsilon=-\infty}^{+\infty} \varepsilon x(n\varepsilon)\delta_\varepsilon(t - n\varepsilon)$, where n is the number of rectangles taken for the approximation. Subsequently the response y_ε becomes $y_\varepsilon(t) = \sum_{n\varepsilon=-\infty}^{+\infty} \varepsilon x(n\varepsilon)h_\varepsilon(t - n\varepsilon)$, with h_ε being the response of the system to δ_ε. By letting ε go to zero we obtain $y(t) = \int_{-\infty}^{+\infty} x(\tau)h(t - \tau)d\tau \equiv x(t) * h(t)$ (Eq.3), where $h(t) = \lim_{\varepsilon \to 0} h_\varepsilon$ is the impulse response of the system to the unit impulse $x(t) = \lim_{\varepsilon \to 0} x_\varepsilon(t) = \delta(t)$. The impulse response is useful because we can obtain the system's complete output calculating (3), known as convolution integral. The notation '$*$' implies that the second function in order is the time-translated one but an important property is the commutativity of the convolution integral i.e. $x(t) * h(t) = h(t) * x(t)$ (Schetzen 2003, 66)

Important system properties

Causality

Causality is the concept of future events being affected by past events and not vice versa. In LTI system theory a system is causal if the output depends only on present and past, but not future inputs. A necessary and sufficient condition for causality is

$$h(t) = 0 \text{ for every } t < 0 \quad (4)$$

where $h(t)$ is the impulse response (Schetzen 2003, 83).

Stability

The definition of stability generally depends on the problem in question and is always considered relatively to some particular concern of the problem. In the context of LTI system theory, stability is expressed in the form of the bounded input-bounded output (BIBO) stability criterion, which says that a system is stable, if its response to a bounded input waveform is a bounded output waveform. Mathematically, if every input satisfying

$$\int_{-\infty}^{+\infty} |x(t)|\, dt = \|x(t)\| < \infty \quad (5)$$

leads to an output satisfying

$$\|y(t)\| < \infty \quad (6)$$

then the system is BIBO stable (Schetzen 2003, 85).

Commutative property

If we connect two LTI systems A and B in a way that the output of the first is the input of the second, the output of the overall system is the same, independently of the order of the systems. Alternatively, the overall impulse response of the system is the convolution

integral of the two separate impulse responses. Fig.3 shows the concept

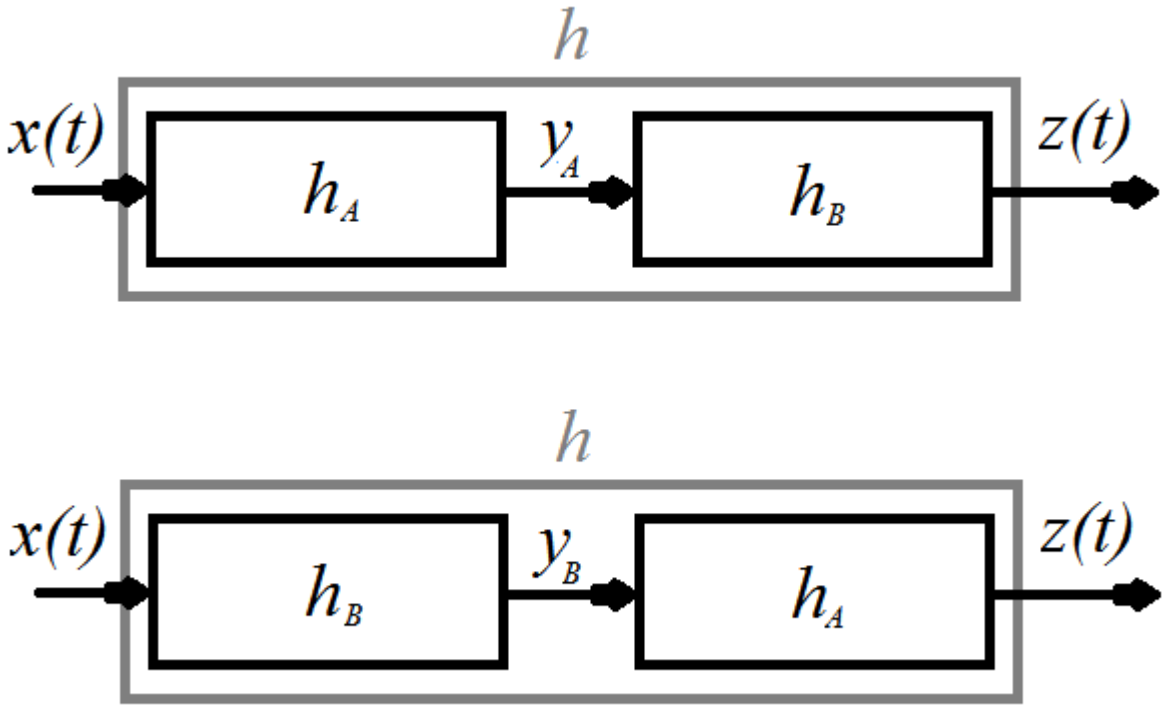

Figure 3: Two connected LTI systems produce the same overall output for the same input, regardless of their order.

This is a consequence of the commutativity of the convolution integral mentioned earlier, i.e. $h = h_A(t) * h_B(t) = h_B(t) * h_A(t)$ (6.1).

The frequency domain approach

The previous discussion involved inputs and outputs as functions of time but the subject can be approached from the frequency point of view as well. Since signals have an equivalent expression in the frequency domain using appropriate transformations, the corresponding analysis can give valuable insight about the behavior of LTI systems.

Eigenfunctions and eigenvalues of an LTI system

For a particular operator, the eigenfunction is the function, who under the operation of said operator, is multiplied by a scalar called the eigenvalue (Bruce R. Kusse 2006, 436). In the context of LTI systems, the operator is the system itself since an input $x(t)$ results in an output of $y(t)$. If the output is the same as the input multiplied by a scalar, then the input signal is an eigenfunction of the LTI system. Suppose the input of the system is $x(t) = Ae^{st}$ with $s, A \in \mathbb{C}$. The output of the system with impulse response $h(t)$ is then:

$$y(t) = \int_{-\infty}^{+\infty} h(t-\tau)Ae^{st}d\tau \quad Eq.7$$

Which by the commutative property of convolution, is equivalent to:

$$y(t) = \int_{-\infty}^{+\infty} h(\tau)Ae^{s(t-\tau)}\,d\tau = \int_{-\infty}^{+\infty} h(\tau)Ae^{st}e^{-s\tau}\,d\tau = Ae^{st}\int_{-\infty}^{+\infty} h(\tau)Ae^{-s\tau}\,d\tau$$

$$= Ae^{st}H(s) \quad Eq.8$$

Where the scalar $H(s) = \int_{-\infty}^{+\infty} h(t)Ae^{-st}\,dt$ (Eq.9), depends only on the parameter s. Since the output scaled version of the input, $x(t)$ is an eigenfunction of the LTI system (in fact, of any LTI system since we used the most general expression of the impulse response) with an eigenvalue $H(s)$. It is important to notice that the LTI system satisfies the BIBO stability criterion since for $x(t)(|x(t)| = |A|)$ the output produced has a norm of $|y(t)| = |A||H(s)|$ (Schetzen 2003, 107).

System response to a step input

If we consider an input $x(t) = E$ for $t \geq 0$ which can be viewed as an exponential with $s = 0$, then Equation 9 becomes $H(0) = A\int_{-\infty}^{+\infty} h(t)\,dt$. $H(0)$ is often called the dc gain of the system (Schetzen 2003, 110) or zero frequency gain and it is the ratio of the steady-state output of the system relative to the magnitude of the step input (Astrom 2008, 239).

Transfer functions

The function $H(s)$ that appeared in the previous section, is called the transfer function of the system and it is of central interest in LTI system theory, since the input and output of the system are connected by the relation $Y(s) = H(s)U(s)$, where $Y(s)$ and $U(s)$ are the Laplace transformations of the output and the input respectively (Alan V. Oppenheim, 1996 p. 693).

Transfer function of a LTI system

By taking the LTI approximation equations 1.1 and 1.2 are modified and give us:

$$\frac{d}{dt}\boldsymbol{x}(t) = \boldsymbol{Ax}(t) + \boldsymbol{Bu}(t), Eq.10.1$$

$$\boldsymbol{y}(t) = \boldsymbol{Cx}(t) + \boldsymbol{Du}(t), Eq\ 10.2$$

Where the functions $\boldsymbol{a}, \boldsymbol{b}$ and $\boldsymbol{c}$ have been replaced by the time-invariant matrices $\boldsymbol{A}, \boldsymbol{B}, \boldsymbol{C}$ plus an additional matrix $\boldsymbol{D}$ to account for the linear dependence of $\boldsymbol{y}$ from $\boldsymbol{u}$. The most general solution to this system of equations is (Astrom 2008, 145)

$$\boldsymbol{x}(t) = e^{\boldsymbol{A}t}\boldsymbol{x}(0) + \int_0^t e^{\boldsymbol{A}(t-\tau)}\boldsymbol{B}\boldsymbol{u}(\tau)d\tau\,, Eq.11.1$$

$$\boldsymbol{y}(t) = \boldsymbol{C}e^{\boldsymbol{A}t}\boldsymbol{x}(0) + \int_0^t \boldsymbol{C}e^{\boldsymbol{A}(t-\tau)}\boldsymbol{B}\boldsymbol{u}(\tau)d\tau + \boldsymbol{D}\boldsymbol{u}(t), Eq.11.2$$

As mentioned before $\boldsymbol{x}, \boldsymbol{y}$ and $\boldsymbol{u}$ can have different dimensions but the matrices have to have the right dimensions to account for the systems dynamics. Therefore, if n is the dimension of $\boldsymbol{x}$, k the dimension of $\boldsymbol{u}$ and m the dimension of $\boldsymbol{y}$, $\boldsymbol{A}$ has to be $n \times n$, $\boldsymbol{B}$ has to be $n \times k$, $\boldsymbol{C}$ $m \times n$ and $\boldsymbol{D}$ $m \times k$. By taking the Laplace transform on both sides of equations 10.1-2, and using the Laplace transform properties (John H. Matthews 1999, 429) we obtain:

$$s\boldsymbol{x}(s) = \boldsymbol{A}\boldsymbol{x}(s) + \boldsymbol{B}\boldsymbol{u}(s), Eq.12.1$$

$$\boldsymbol{y}(s) = \boldsymbol{C}\boldsymbol{x}(s) + \boldsymbol{D}\boldsymbol{u}(s), Eq.12.2$$

Where $s = \sigma + i\omega$ is the Laplace variable. We can derive the ratio $\frac{y(s)}{u(s)}$ and the transfer function is:

$$\boldsymbol{G}(s) = \frac{y(s)}{u(s)} = \boldsymbol{C}(s\mathbb{I} - \boldsymbol{A})^{-1}\boldsymbol{B} + \boldsymbol{D}, Eq.13$$

For the special case of an exponential input $\boldsymbol{u}(t) = e^{st}$, $\boldsymbol{y}(t) = \boldsymbol{G}(s)\boldsymbol{u}(t)$ (Astrom 2008, 233). An important property of the transfer function is its commutativity in the case of two connected LTI systems. This is because of the convolution theorem that states that the Laplace transform of a convolution integral is simply the product of the Laplace transforms of the functions involved in the convolution (John H. Matthews 1999, 429).

The figure below illustrates this concept.

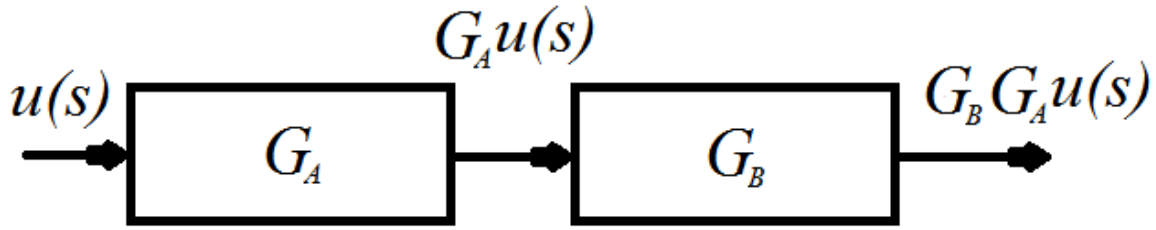

Figure 4: When two systems are connected with a common signal, their transfer functions can be multiplied to give the transfer function of the composite system.

Feedback

The process of applying a control input in order to affect the output of a dynamical system, that has been described in the previous sections, can be classified based on the control input's relation to the output. Open-loop control is when the control action (and therefore the input $\boldsymbol{u}(t)$) is independent of the output $\boldsymbol{y}(t)$ (Joseph DiStefano, 1990 p. 3). Closed-loop control on the other hand, is the type of control, in which the control action is, in some way, dependent on the system's output (Joseph DiStefano, 1990). This type of control is commonly known as feedback control. Feedback is some way of comparing the output of the system, to the input, in order to produce a control action which can be a function of both the input and the output (Joseph DiStefano, 1990).

Transfer function of a closed-loop system

Below is a figure showing a typical closed-loop system, i.e. one that uses feedback in order to control the process (called a feedback controller for obvious reasons).

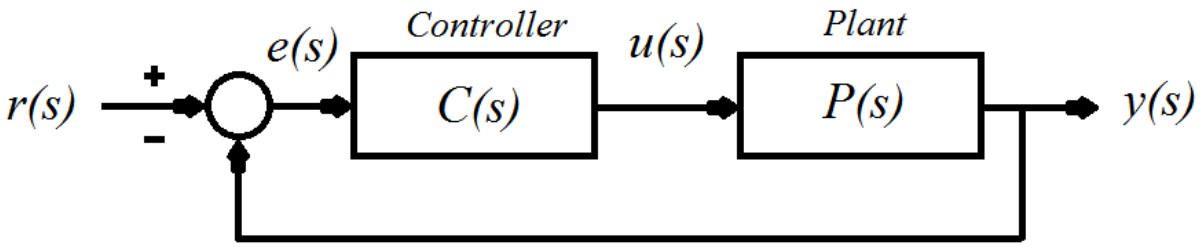

Figure 5: Flow diagram of a process controlled by a feedback controller. A reference signal r(s) is fed to the controller, which compares it to the output y(s) and creating an error signal e(s). The controller produces the control signal u(s) that aims to minimize e(s).

The transfer function of the controller is $C(s)$ and the plant's is $P(s)$. The quantity $r(s)$ is the reference signal and is the representation of the desired value of the process to be controlled and $y(s)$ is the overall output of the system, while $e(s)$ is the error signal, i.e. the difference of the output and the reference.

Following the discussion about transfer functions of LTI systems, the transfer function of a closed-loop system can be found to be:

$$T(s) = \frac{y(s)}{r(s)} = \frac{P(s)C(s)}{1 + P(s)C(s)}, Eq.\,14$$

Since $u(s) = C(s)e(s) = C(s)(r(s) - y(s))$ and $y(s) = P(s)u(s) = P(s)C(s)e(s) = P(s)C(s)(r(s) - y(s))$, with some algebraic manipulation we arrive at Equation 14.

Types of feedback control

Proportional control

Proportional control consists of taking the $\boldsymbol{u}$ term in Equations 10.1-10.2 be proportional to the error signal i.e. $\boldsymbol{u}(t) = -\boldsymbol{K_c}(\boldsymbol{r}(t) - \boldsymbol{y}(t))$. The controller interprets the error signal and minimizes by implementing a proportional and inverse signal. A controller of this type has the transfer function $\boldsymbol{C}(s) = \boldsymbol{K_c}$. $\boldsymbol{K_c}$ is known as the proportional gain (Willis 1999, 2) and is not to be confused with the dc gain mentioned earlier. A proportional-only controller will typically reduce $\boldsymbol{e}(t)$, but an offset will continue to exist if it is not calibrated near the set point $\boldsymbol{r}(t)$ (Willis 1999, 2).

Proportional-Integral control

In this type of control the control signal is $\boldsymbol{u}(t) = \boldsymbol{K_c}\boldsymbol{e}(t) + \frac{\boldsymbol{K_c}}{T_i}\int_0^t \boldsymbol{e}(t)dt$, with the corresponding transfer function being $\boldsymbol{C}(s) = \boldsymbol{K_c} + \boldsymbol{K_c}/T_i s$ (Willis 1999, 3) which compared to the proportional-only control signal has an extra term proportional to the integral of the error signal over time, with T_i being a parameter known as integral time. The integral term reduces the offset that might occur using a proportional-only controller, by taking into account the value of $\boldsymbol{e}(t)$ at earlier times (Willis 1999, 3).

Proportional-Integral-Derivative control

Here the control signal is $\boldsymbol{u}(t) = \boldsymbol{K_c}\boldsymbol{e}(t) + \frac{\boldsymbol{K_c}}{T_i}\int_0^t \boldsymbol{e}(t)dt + \boldsymbol{T_d}\frac{d\boldsymbol{e}(t)}{dt}$, with a transfer function $\boldsymbol{C}(s) = \boldsymbol{K_c} + \frac{\boldsymbol{K_c}}{T_i s} + \boldsymbol{T_d}s$ (Willis 1999, 4). The additional term predicts the behavior of the process, by looking at the rate of change of the error, hence its dependence on the derivative. The parameter $\boldsymbol{T_d}$ is called the derivative time. The parameters $\boldsymbol{K_c}, T_i$ and $\boldsymbol{T_d}$ are the ones one needs to specify in a real controller in order to effectively control a process. Often in commercial controllers, the proportional gain is

replaced by the proportional band PB (as was the case with the controller used in this thesis). The relation between the proportional gain and the proportional band is $PB = 100\%\frac{1}{K_c}$ (Willis 1999).

Tuning methods

Tuning is the process of determining the optimal values for the K, T_i and T_d parameters of the actual controller, depending on the given system. Optimal in this context, means the values for which the system becomes as stable as possible or in other words, the error's $e(t) = r(t) - y(t)$ norm is kept at a minimum. Although a theoretical approach of the problem is possible, practical methods are more direct and provide acceptable stability to the system, with little knowledge of the systems properties. The methods developed by Ziegler and Nichols (J.G. Ziegler 1942) are the most widely used and rely on the calculation of few parameters to characterize the system. The advantage of these empirical methods is that they can be utilized by non-expert personnel to tune a controller.

Ziegler-Nichols methods

1. The step response method

One method introduced by Ziegler and Nichols is obtaining information by implementing a step input into the system in question. The I and D values of the controller are set to zero, leaving only the gain P. The step input is on until the process variable (in our case temperature) becomes stable (or relatively stable). The point where the slope of the step response has its maximum is first determined, and the tangent at that point is drawn. The intersections between the tangent and the coordinate axes give the parameters a and L that characterize the system's step response as seen in figure. The P, I and D values are then given by the table below (J.G. Ziegler 1942).

Controller	K	T_i	T_d
P	$1/a$		
PI	$0.9/a$	$3L$	
PID	$1.2/a$	$2L$	$0.5L$

Table 1.1: Corresponding controller values for the step response method

2. The frequency response method

This method (which was used in our case) involves setting all the controllers values to zero and then slowly increasing the gain, until the system's response, starts to oscillate. The gain when this occurs is K_u and the period of the oscillations are T_u. By measuring T_u we can then determine the I and D values that are given by tables (J.G. Ziegler 1942). The frequency response method can be viewed as an empirical tuning procedure where

the controller parameters are obtained by direct experiments on the process combined with some simple rules.

Controller	K	T_i	T_d
P	$0.5K_u$		
PI	$0.4K_u$	$0.8T_u$	
PID	$0.6K_u$	$0.5T_u$	$0.12T_u$

Table 1.2: Corresponding controller values for the frequency response method

In our PID controller the proportional band is used (PB) which is the inverse of the gain K, therefore the table values would also be inversed.

Chapter 4 Stabilizing the temperature on the experiment

In this chapter the experimental setup and procedure with which the temperature was stabilized is described.

Position of the problem

The problem we were trying to solve was the excessive fluctuation in temperature inside the experiment box due to the air-conditioning (A/C) unit's limited stabilization abilities. The A/C unit was displaying a number of different "behaviors", at different times of the day, but the most common was an oscillation of the temperature around the A/C set point, with an amplitude of approximately ±0.1°K. Below is a typical plot of these oscillations over the course of a few days.

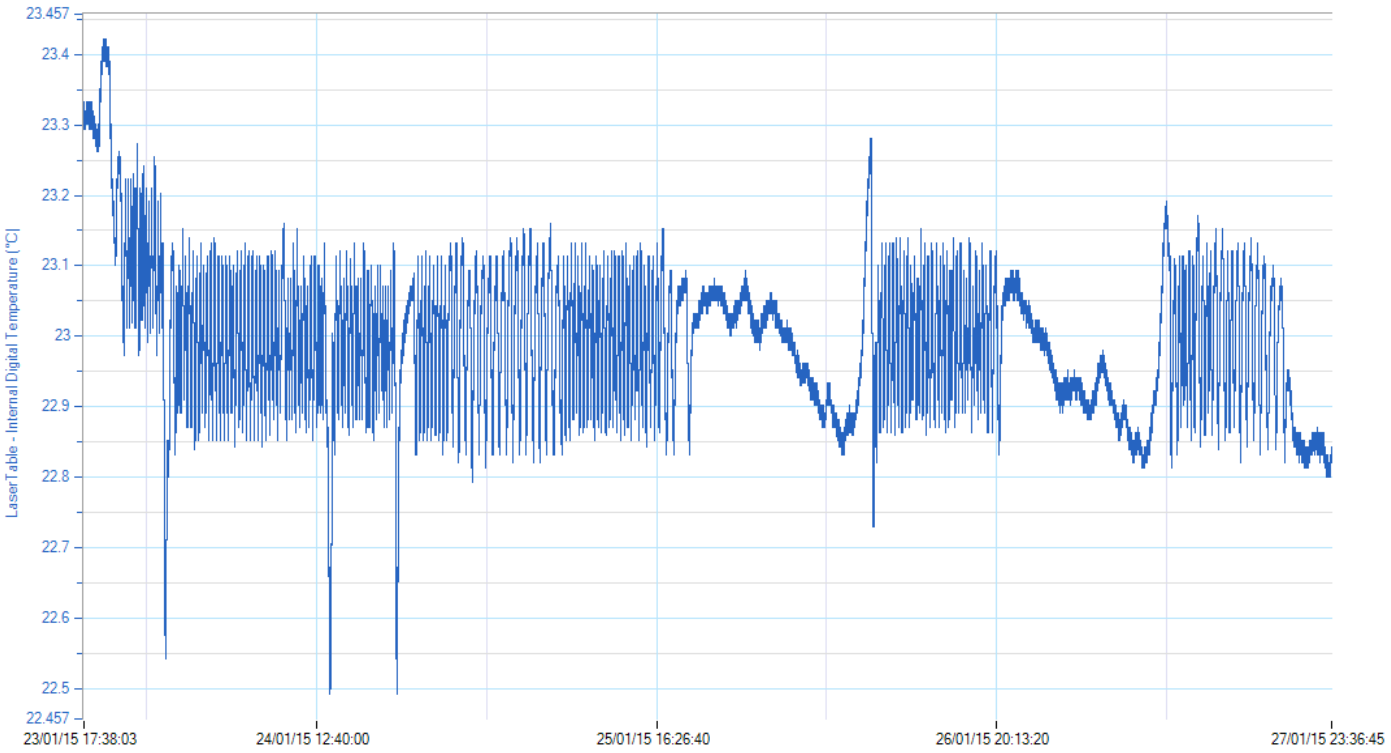

Figure 6: Temperature fluctuations inside one of the experiment boxes of the lab. The change in the frequency of the oscillations and the typer of drift are due to pauses in the experimental equipment.

As mentioned earlier, big fluctuations in temperature can cause a number of problems, including misalignments in optical components, which ultimately lead to a fluctuation in the number of atoms in the MOT. Our goal is to build a simple stabilization system that can mitigate the big drops in temperature in the short term and keep the temperature near a fixed value in the long term without letting it slowly drift downwards.

Thermometer Characterization

Before using the thermometers to measure the surrounding temperature, they were characterized in order to be able to make a sensible interpretation of the data. The two Microlite thermometers use a 10K NTC thermistor as temperature sensor. Both have $\pm 0.3°K$ accuracy and $\pm 0.03°K$ resolution in temperature and a maximum sampling rate of 1 point per second. The DT304 thermometer uses four K-type thermocouples with an accuracy of $\pm(0.1\% + 0.5°C)$ of the temperature reading, which for the range of temperature the experiment is operated at, translates to an accuracy of ±0.5°C and a resolution of 0.1°C. They were characterized by heating them up with a heat gun and then let to reach equilibrium with the surrounding environment. The temperature data was then collected using the associated software. This procedure was done inside a thermally insulated box to avoid external disturbances. The temperature data was then fitted using OriginLab and the thermometers' time constants were deduced. The fitting function used for all cases was $y(x) = A_1 e^{-t/\tau} + y_o$, where A_1 and y_o are constants, corresponding to the temperature difference, t is time and τ the time constant we are interested in.

LITE5032P-RH-A

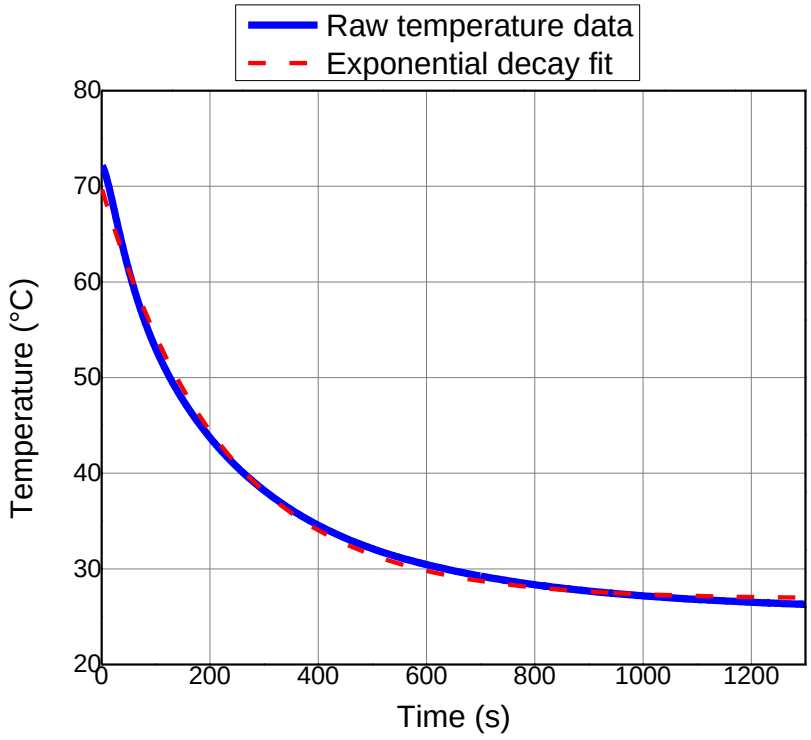

Figure 7.1:Temperature data and corresponding fit for the LITE5032P-RH-A thermometer

Fit Results

Parameter	Value	Standard error

$A_1(°C)$	43,00	0,03
$y_o(°C)$	26,86	0,09
$\tau\ (s)$	224	1
$1/\tau\ (s^{-1})$	0,00447	$1{,}81374 \cdot 10^{-5}$
$\tau_{½}(=\tau ln2)$	154,96132	0,62834

LITE5032P-A

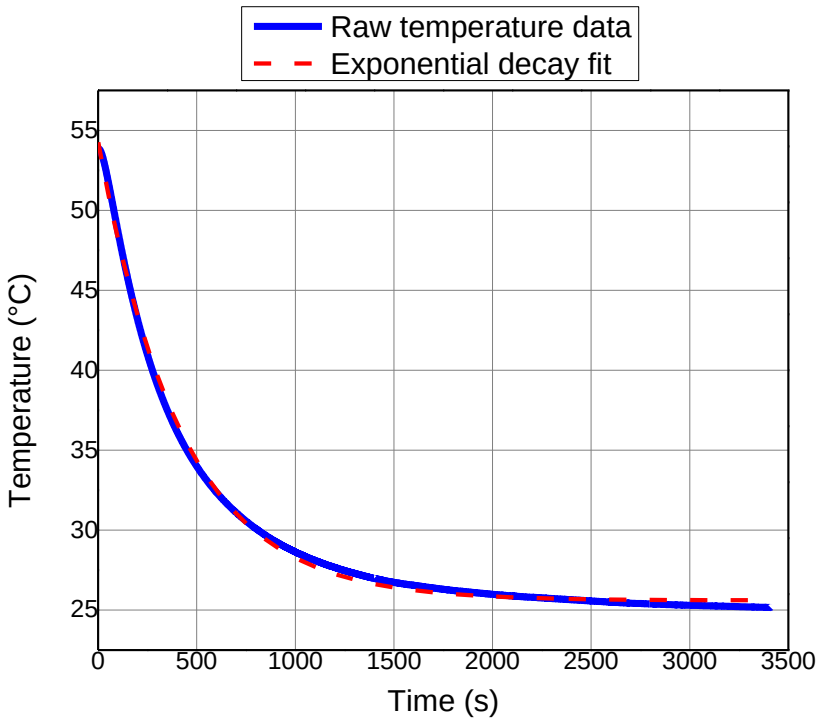

Figure 9.2: Temperature data and corresponding fit for the LITE5032P--A thermometer

Fit Results

Parameter	Value	Standard error
$A_1(°C)$	28.72	0.03
$y_o(°C)$	25.60	0.01
$\tau\ (s)$	421	1
$1/\tau\ (s^{-1})$	0.01	0.01
$\tau_{½}(=\tau ln2)$	291.55	0.54

DT304

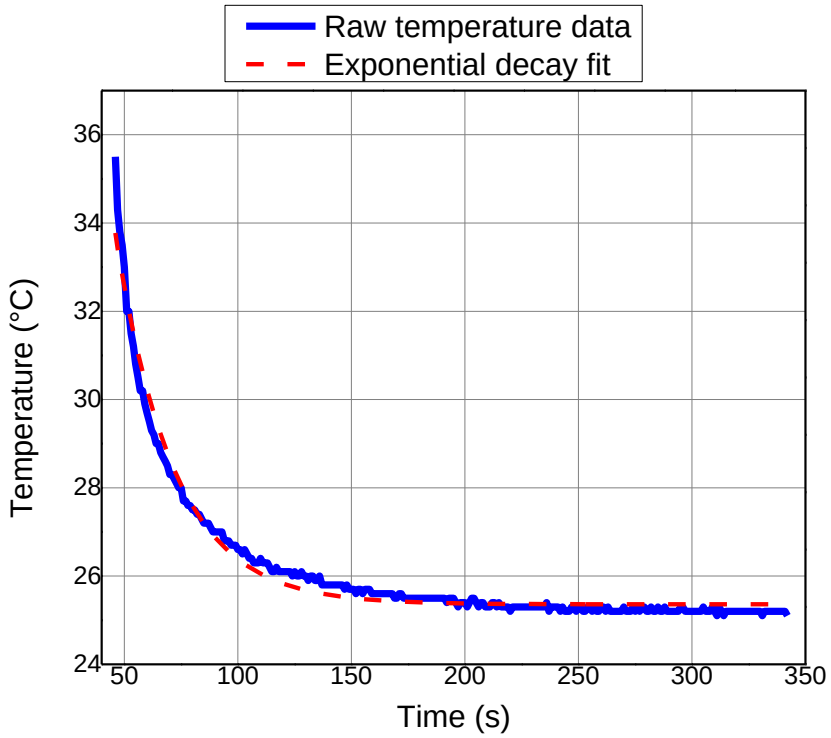

Figure 8: Temperature data and corresponding fit for the DTC304 thermometer

Fit Results

Parameter	Value	Standard error
$A_1(°C)$	50.69	1.95
$y_o(°C)$	25.36	0.02
$\tau\ (s)$	25.61	0.44

$1/\tau\ (s^{-1})$	0.04	0.01
$\tau_{½}(=\tau ln2)$	17.75	0.31

- *Comments*

The fitting gives rather long time constants for the two Microlite thermometers, of the order of minutes. Typically 10K NTC thermistors have time constants of the order of seconds (tdk.eu n.d.). However the Microlite thermometers, indeed, showed a slow time response when monitoring the temperature with the DataSuite software. For this reason the Microlite thermometers were used for observing changes in temperature. For any application involving time (such as tuning the controller), DT304 was used due to its much better time response (26 seconds compared to 223 and 420).

The BEC1 box as an LTI system

Before tuning the controller we assessed whether the plant we want to control is indeed a first-order system or there are second order phenomena we need to take into account. This is done by utilizing the step response method, while the air-conditioning system was on, and observing the temperature's response. To do that, the PID controller's integral and derivative time were set to zero and the proportional band was set to its lowest possible value (0.01). The set point of the PID was then set at a much higher temperature than the ambient around the sensor, in order to have constant (maximum) power from the heating wire, up to the point where the air near the MOT reached a steady-state condition. This was done for all three of the fan's speeds although the experiment mostly operates under the highest fan speed. Based on the discussion in Chapter 3, a first-order-system's transfer function (the Laplace transform of the linear equations 10), must be of the form $(s) = \frac{y(s)}{u(s)} = \frac{K}{\tau s+1}$, where K, is the static gain of the system and τ, is the system's time constant (time needed for the temperature to reach 63% of the steady-state value). As the system's output y we consider the difference between the (average) initial and the (average) steady-state temperature $\Delta T(t)$, and as its input, the time that the heating wire is on (i.e. duty cycle). By finding the static gain K and the time constant τ, we find $P(s)$ and check how well it fits our data.

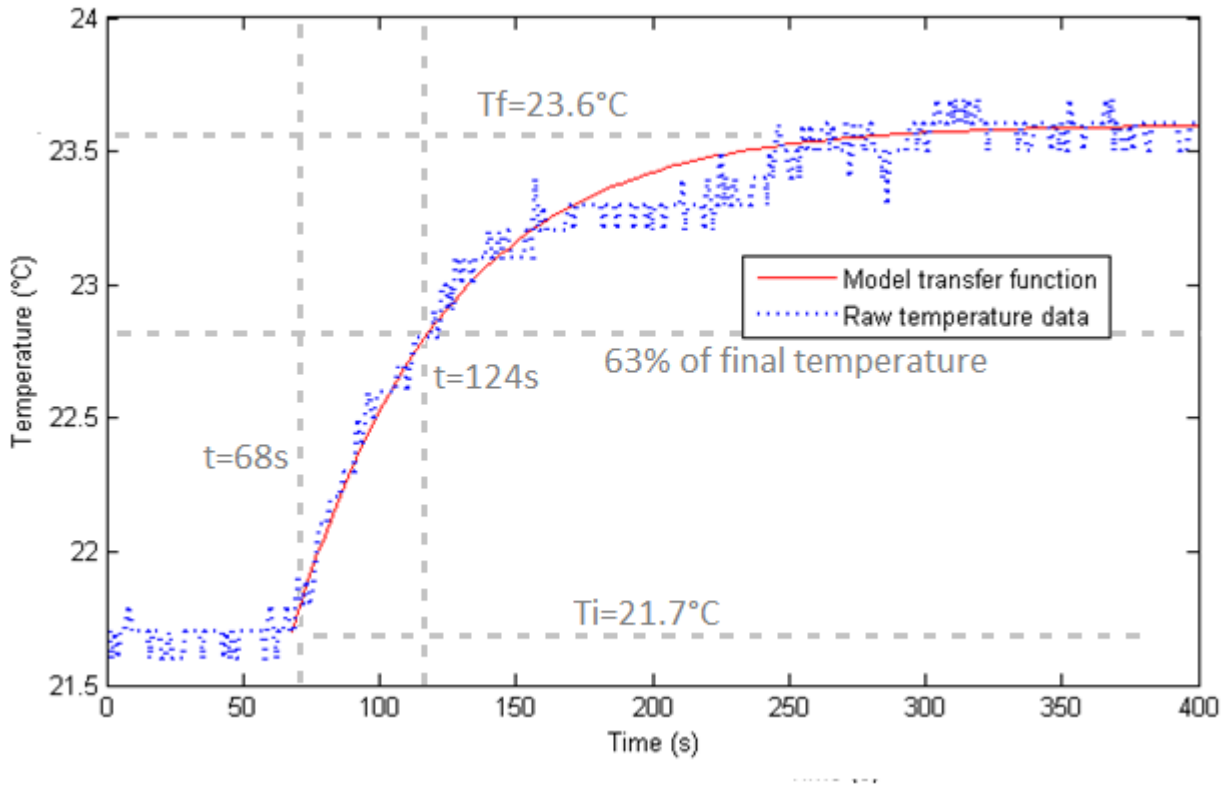

Figure 9: Raw temperature data of the BEC1 box with a step-input implemented (blue). The measured time constant is 56s and the static gain is 1.9°C. These values where used for the first order transfer function (red) that was fitted to the data.

From inspection of the graph above we see that $\tau = 56s$ and $K = 1.9℃$ therefore the first-order transfer function is $P(s) = \frac{1.9}{56s+1}℃$ and is represented by the red line on the graph. We can see that out assumption of a first order system is reasonable as the model function fits quite well to the experimental data.

First attempt at a stabilization system

The first attempt at a temperature stabilization system, was done by using a digital PID controller, which controlled a set of four incandescent light bulbs to heat the incoming air. The PID controller used was an Omron E5CN-HT, which was powered by the 220V mains voltage. It uses a platinum resistance thermometer as a temperature sensor and has $\pm 0.1°K$ temperature resolution and an accuracy of ±0.1% of the displayed process value, as well as an input sampling period of 60ms. It produces a 0-12V control voltage, normally used for driving a solid-state relay (SSR). However, as the SSR's output is too high for the lamps that were used(5A output SSR, was the lowest possible available to use with our controller), we opted to use the controller's control voltage to control a Delta Elektronika ES 030-10 power supply with 0-30V and 0-10A output which gives a

maximum power output of 300W. The power supply's electrodes were then connected to the set of four 100W-24V halogen light bulbs. By using Ohm's law for power

$$P = \frac{V^2}{R}\ , Eq.16$$

and solving for resistance we find that each lamp has a 5.76Ω resistance. It is obvious that we could not use all 400W of the four lamps' power, therefore, the lamps were all wired in parallel, giving a 1.44Ω resistance, in order for the overall resistance to be close to 3Ω, which gives us the maximum output power out of the power supply. The reason we chose to spread the 300 Watts of the power supply across four lamps (and not three of overall maximum power of 300W), is because we wanted multiple heat sources in order to heat the incoming air more efficiently. The lamps were placed inside the duct, above the HEPA filter and one of the thermometers, connected to a computer was placed under the HEPA filter to monitor the temperature. The schematic below shows the configuration. Table show the controller's possible values.

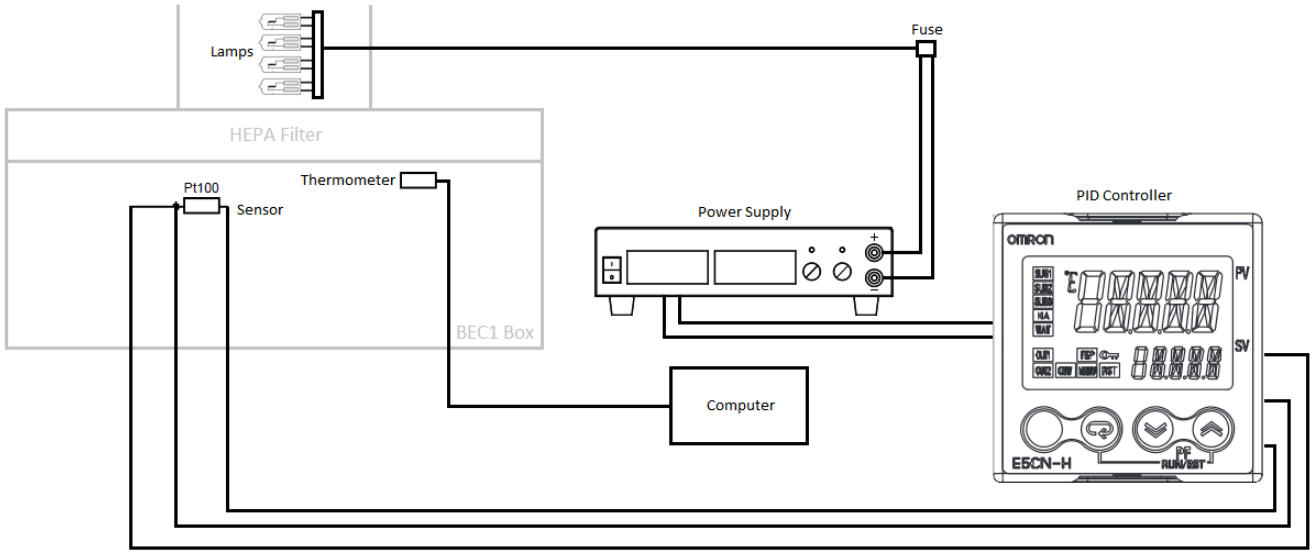

Figure 10: The first stabilization system

Value	Range	Units
Proportional Band (P)	0.1 -3,240.0	℃
Integral Time (I)	0.0-3,240.0	seconds
Derivative (D)	0.0-3,240.0	seconds

To tune the controller, the frequency response method was used. The values of integral time (I) and derivative time were set to zero and the proportional band (PB) was increased from 0.1℃ up to a value that the temperature under the HEPA filter started to

oscillate. The set point was 22.5℃ and the temperature was monitored using the DT304 thermometer. After measuring the average period of the oscillations by inspecting the temperature's graph, the P, I, and D values were set according to Table 1.2. The P value at which the system started to oscillate was 0.3℃. The figure below shows the oscillations of the temperature.

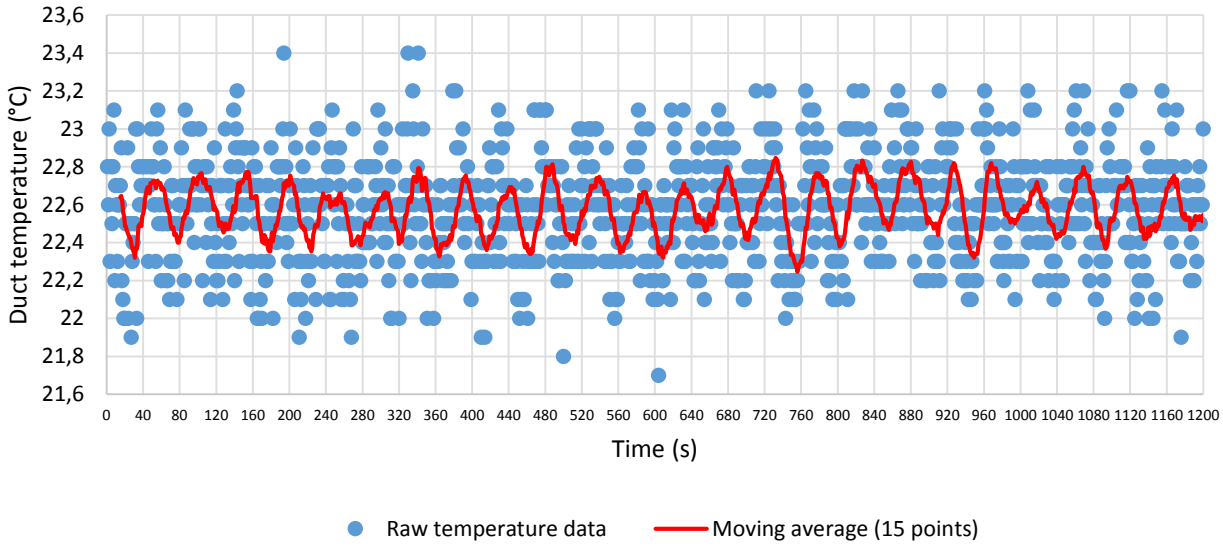

Figure 11: Temperature oscillations during implementation of the frequency response method.

The average period of these oscillations was calculated at 49±7 s, therefore, using Table 1.2 we get the values $P = 0.3℃,\ I = 24.5 \pm 4\ s, D = 5.9 \pm 0.8\ s$.

Stabilizing the temperature

As soon as the optimal P, I and D values were determined, the stabilization system was put to the test. The set point (SP) of the PID controller was set at 22.8℃, while the set point of the air-conditioner (A/C) was set at 21.9℃. The A/C is capable of holding the temperature within ΔT=±0.3℃ of its designated set point, therefore, we were looking at a maximum actual temperature of 22.2℃ and a minimum of 21.6℃. With the 300W of the light bulbs available, according to Equation, for the maximum fan speed, we expect a maximum increase in temperature of 0.4±0.5 ℃. It should be noted that there is an offset between the A/C temperature sensor and the thermometer used, but since we are interested in temperature differences this offset is eliminated in the final results. The temperature data under the HEPA filter, before and after the PID controller is turned on, is shown in the figure below.

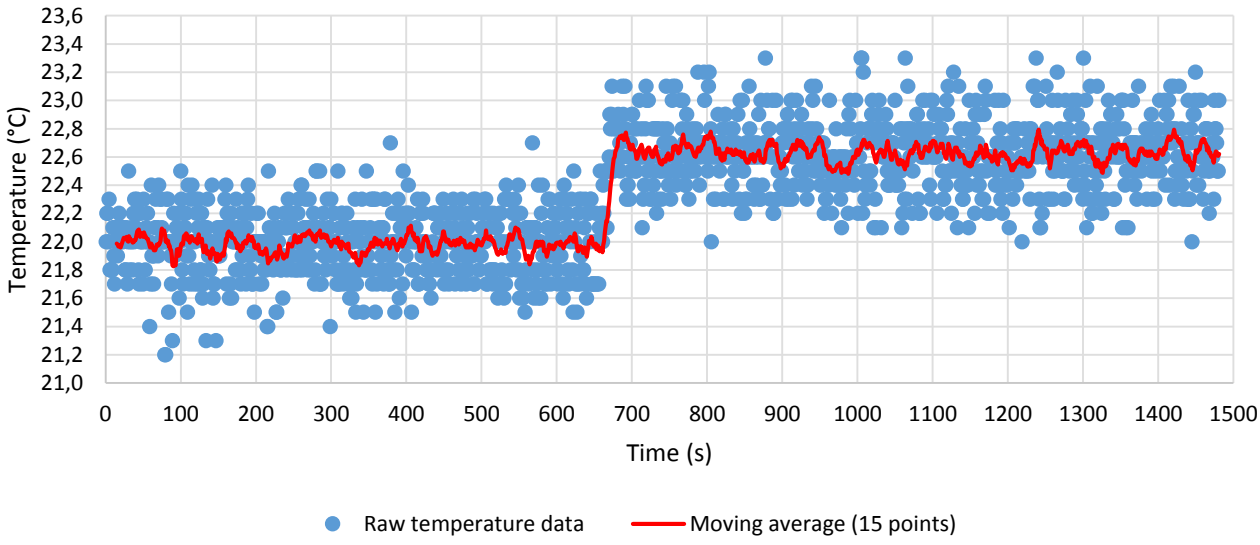

Figure 12: Temperature data before and after the stabilization system is turned on.

Before the PID controller is turned on (the time interval from 0s to about 650s) the average temperature is 22.0±0.5 °C , whereas after turning on the PID (from about 700s and onwards), the average temperature is 22.4±0.5 °C. The difference in temperature is 0.4±0.5 °C, in accordance with the theoretical prediction. Since we are interested in examining whether or not the stabilization system mitigates the problem of large fluctuations in air temperature, we should compare the standard deviation of the temperature, before and after the stabilization process. However, our estimate of the short-term fluctuations is limited by the accuracy of the thermometer used, which is ±0.5°C. For the record, the standard deviation before the stabilization was 0.2°C, the same as after. Thus, we can only examine whether it can keep the temperature from slowly drifting during long periods of time. We do that by breaking down the time series of the temperature into segments of 500 points and looking at the average of each segment. This analysis is done after point #2000, because that is when the temperature settles down from the initial overshooting that occurs just after turning on the PID controller. Below is a table summing up the measurements.

Segment (point #)	Average temperature (°C) ±0.5
2000-2499	22.5
2500-2999	22.5
3000-3499	22.5
3500-3999	22.5
4000-4499	22.5
4500-4999	22.5

Table 2: Average temperature of consecutive 500-point segments of the temperature time series.

As we can see, the PID controller does well at keeping the temperature at a fixed value over long periods of time (in this case a little under 1.5 hours).

Conclusions

We saw that the first stabilization system that we built did well at keeping the temperature near a fixed value but the limited accuracy of the thermometer that was available at the time did not allow us to assess whether the fluctuations around that fixed value were actually less than before implementing it. Also, we observed that the rise in temperature when the system was at work, was consistent with our theoretical prediction. Although our first stabilization system, performed well by holding the temperature at a fixed value, we decided to build a new one. The main reason for this was our PID controller's low resolution (0.1°C) which would make the task of controlling the fluctuations down to the 0.01°C limit difficult. Therefore, we replaced the Omron PID controller, with one of higher resolution. We also decided to replace the light bulbs, and find something more efficient as a means of heating the incoming air, since they were quite small in size, with little surface area. We describe the new stabilization system in the following section.

Overview of the new stabilization system

The new stabilization system consists of four main components:

1) A Eurotherm 2416 PID controller
2) A Crydom MCPC2450 control relay
3) A Delta Elektronika ES 030-5 power supply
4) An insulated heating wire of 123.1Ω resistance wrapped around a metal panel

The PID controller is powered by the 220VAC line and uses a Pt100 platinum resistance thermometer as a temperature sensor. It has ±0.01°C accuracy in temperature display. It gives a control output of 4-20mA which controls the control relay. The control relay is powered by the 0-30V power supply and is connected to the mains voltage. Depending on the amount of current the relay receives from the PID controller, it lets a corresponding amount of mains voltage created on the ends of the heating wire with a maximum of 220V (100% of the mains voltage)as in figure 15.2, therefore (using Ohm's law $P = \frac{V^2}{R}$) having a maximum power of 793W. The temperature inside the the BEC1 case was measured using two Fourtec Microlite thermometers (models LITE5032P-A temperature logger and LITE5032P-RH-A temperature and humidity logger). Also a third thermometer (UEI Apollo DT304) was used for tuning the PID controller using the frequency response method. The schematic below shows the configuration of the

stabilization system.

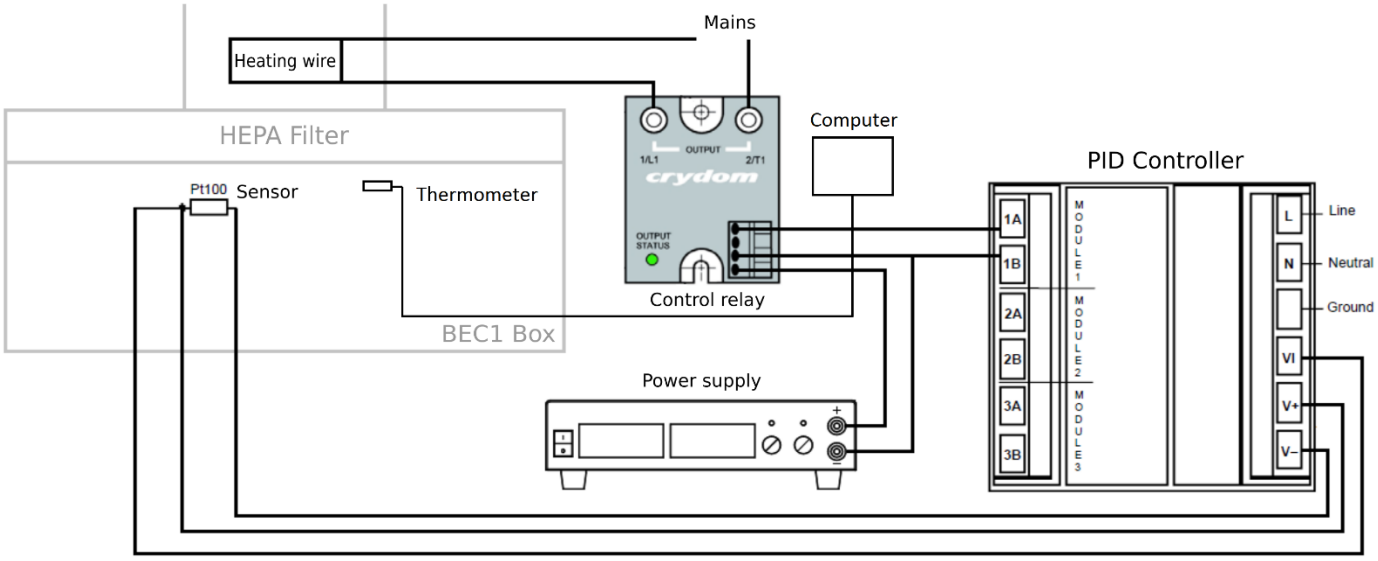

Figure 13: Configuration of the stabilization system

1. The PID controller

The PID controller is a Eurotherm 2416 digital temperature/process controller. It is powered by the 220V mains voltage. It has a DC current control output from 4mA to 20mA. For temperature input, a Pt100 platinum resistance thermometer is used. A layout of the controller's rear terminals is shown in fig below

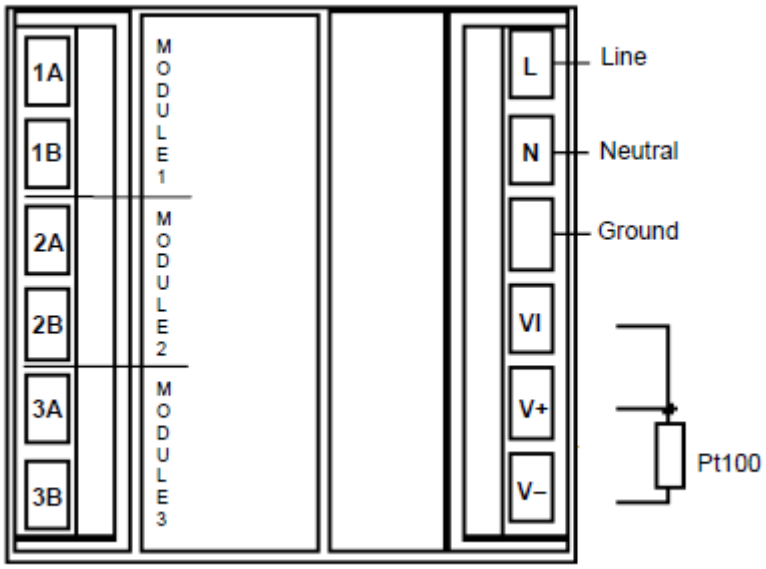

Figure 14:Real terminal layout of the PID controller

The electrical and sensor connections are on the right. From the three modules shown in the picture, Module 1 provides the control output and is connected to the control relay. The controller was used in its automatic mode in which the power is automatically adjusted to maintain the temperature at the set point.

2. The control relay

The control relay used is a Crydom MCPC2450. It is a microprocessor based solid-state relay. It uses a 4-20mA current control input and a produces 0 to 50A output. A 8-32V

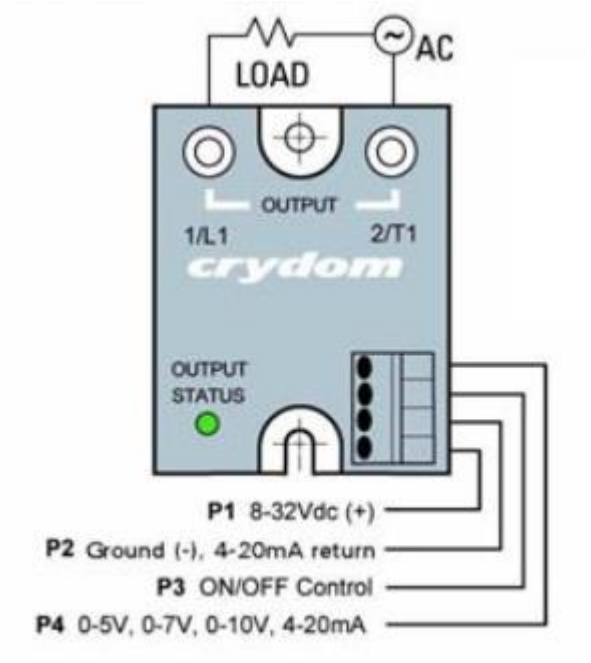

Figure 15.1: Electrical connections for the control relay.

Figure 15.2: True RMS voltage output (percentage of mains voltage) versus analog input signal current (mA).

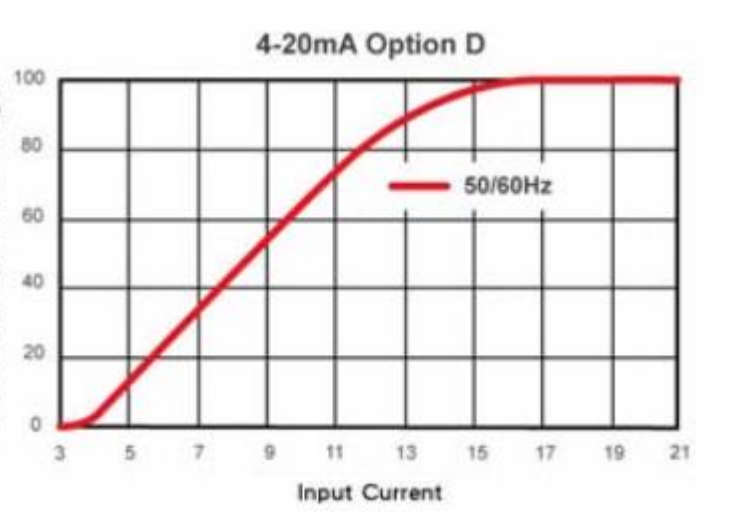

power supply is needed to power the device, so a Delta Elektronika ES 030-5 was used. The relay was screwed onto a piece of aluminum to use as a heat sink, to avoid overheating. The relay uses the 220V mains voltage in order to achieve the 50A output, depending on the control input that it receives from the PID controller, in accordance with the figure below, provided by the manufacturer. An outlay of the relay's electrical connection is also provided.

The relay is connected to a load, which in our case is the insulated heating wire that provides the heating for the experiment.

Principle of operation

The heating wire was placed inside the air duct just over the HEPA filter in order to heat the incoming air and damp the fluctuations that are caused during the stabilization from

the air-conditioning system. Assuming steady-state conditions (all of the heat from the heating wire is transferred to the air whose temperature we want to control), the power need to change the temperature would be

$$P = A\rho vc\Delta T, \textit{ Eq. 17}$$

Where A is the surface area of the HEPA filter, through which the air is distributed, ρ is the density of air, v is the velocity of the air coming through the HEPA filter which is determined by the fan speed selected from the A/C unit, c is the specific heat capacity of air and ΔT is the change in temperature. Inserting values for the known parameters of the equation, we get the expressions

$$P_1 = (795.4 \pm 210.1)\Delta T\ Watts, \textit{ Eq. 18.1}$$

$$P_2 = (620.6 \pm 26.2)\Delta T\ Watts, \textit{ Eq. 18.2}$$

$$P_3 = (454.5 \pm 13.9)\Delta T\ Watts, \textit{ Eq. 18.3}$$

for the three different fan speeds, with 1 being the high fan speed, 2 being the medium and 3 being the low. The density of air at room temperature (approximately $20°C$) is considered to be $1.204\ kg/m^3$ (Eng) and the specific heat capacity is $1.005\ kJ/kg°K$ (Eng). The surface area of the HEPA filter was measured at $0.7 \pm 0.1\ m^2$. Most of the uncertainty in the calculation of the needed power, comes from the measurement of the air speed for the three different fan speeds. The way this was done, was by letting a small piece of paper fall from under the HEPA filter and measuring the time it took to reach the experiment table. These measurements gave the values $(0.9 \pm 0.2)\frac{m}{s}$, $(0.7 \pm 0.1)\frac{m}{s}$, $(0.5 \pm 0.1)\frac{m}{s}$ from highest to lowest fan speed. Despite the large error in the calculation (mostly of P_1), the power provided by the heating wire is well into the desired range for drops in temperature of the order of up to $10^{-1}°K$, which are the ones we are trying to mitigate.

Ideally, the system would not only use heating as a way to control the temperature but cooling as well (by controlling the intake of room temperature air with a small fan as in Dedman 2015 for instance), but the aim was to create something efficient, with readily available parts, and with as less disturbing of the experiment environment as possible. The heating wire has been chosen because, as demonstrated before, can have a large power output and therefore can handle big drops in temperature. Additionally, when wrapped around the metal frame, it provides a large surface area so that the incoming air can be more efficiently heated. The temperature sensor of the PID controller was placed directly under the HEPA filter in order to get the feedback and the sensor of the A/C unit was placed far away from the heating wire in order to avoid any feedback from it (which

would cause the A/C to try to counter the local temperature rise and this in turn would cause the response of the PID controller and so on). Because the stabilization system, as mentioned before, has only the capability of heating the incoming air, the set point was set at ~0.5-1°C above the A/C induced temperature. If the set point of the PID controller was chosen to be the same as the one of the A/C unit, overshooting of the temperature would occur, since once the temperature exceeded the set point of the PID controller, it would stop the heating process and the A/C would continue the oscillation of the temperature that we are trying to reduce. By choosing a set point which differs from the A/C set point by as much as the magnitude of the intrinsic A/C fluctuations, we avoid the constant overshooting and we achieve better thermal stability. Some overshooting occurs, but that is the normal overshooting that takes place during the stabilizing of the control loop and is to be expected.

Tuning the controller

In order to tune the PID controller the frequency response method was used, mentioned in Chapter 4. The controller's proportional band was set to the lowest possible value (0.01) and was gradually increased, until the air temperature started to oscillate, which happened for P=0.13. The air temperature in this case was measured inside the duct and not under the HEPA filter and was monitored using the DT304 thermometer because of its faster time response. The temperature was then let to do a few oscillations and after those were complete, the average period was calculated by measuring the time directly on the temperature-time graph. This procedure was performed only for the highest fan speed since the experiment always operates under the highest speed. Below is the temperature-time graph showing the oscillations.

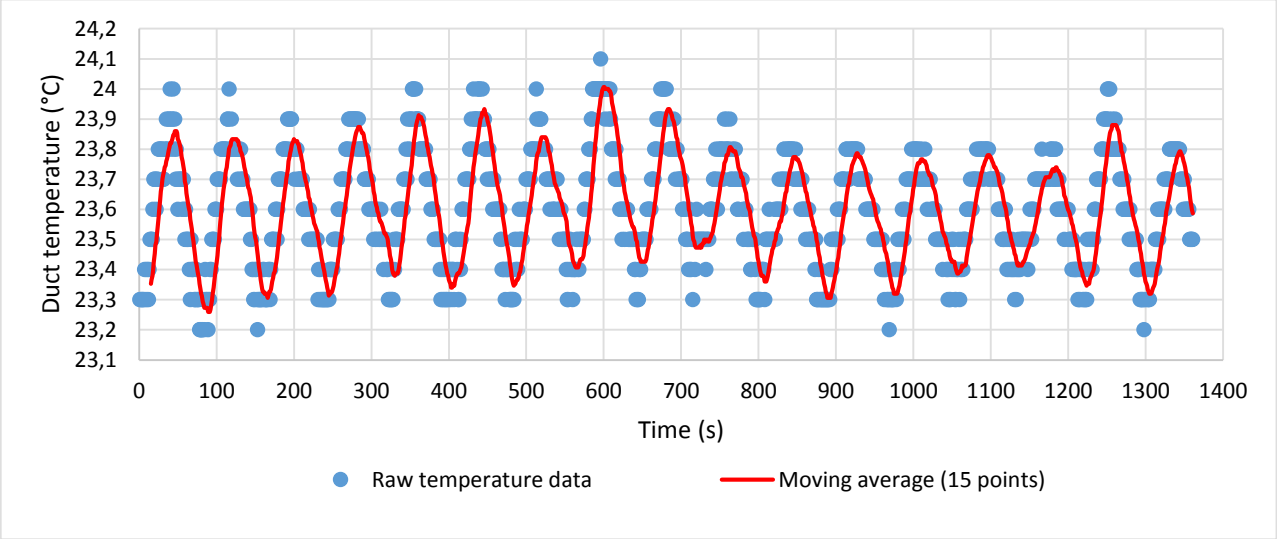

Figure 16: Temperature oscillations induced by the frequency response method, to evaluate PID values for the new stabilization system.

The average period of these oscillations was calculated at 81±5 s, therefore, using Table 1.2 we get the values $P = 0.08,\ I = 40.5s, D = 9.72s$.

- *Comments*

Although the values given by the calculation work well, the system responds well for a range of values, and the proportional band was actually fine-tuned with a little trial and error.

Testing the stabilization system

Using the PID values obtained by the Ziegler-Nichols method we tested the stabilization system inside the BEC1 box. The A/C temperature was set to 22.9 °C and the PID controller was set at 23.34 °C. The temperature for the testing was measured under the HEPA filter. It should be noted that the A/C unit's sensor, which normally is inside the BEC1 box, was moved far away and in the duct. This was done to avoid any feedback from the A/C unit's operation onto the PID and vice versa. The graph below shows the temperature for a period of about seven hours. The temperature data were gathered using the Microlite thermometer.

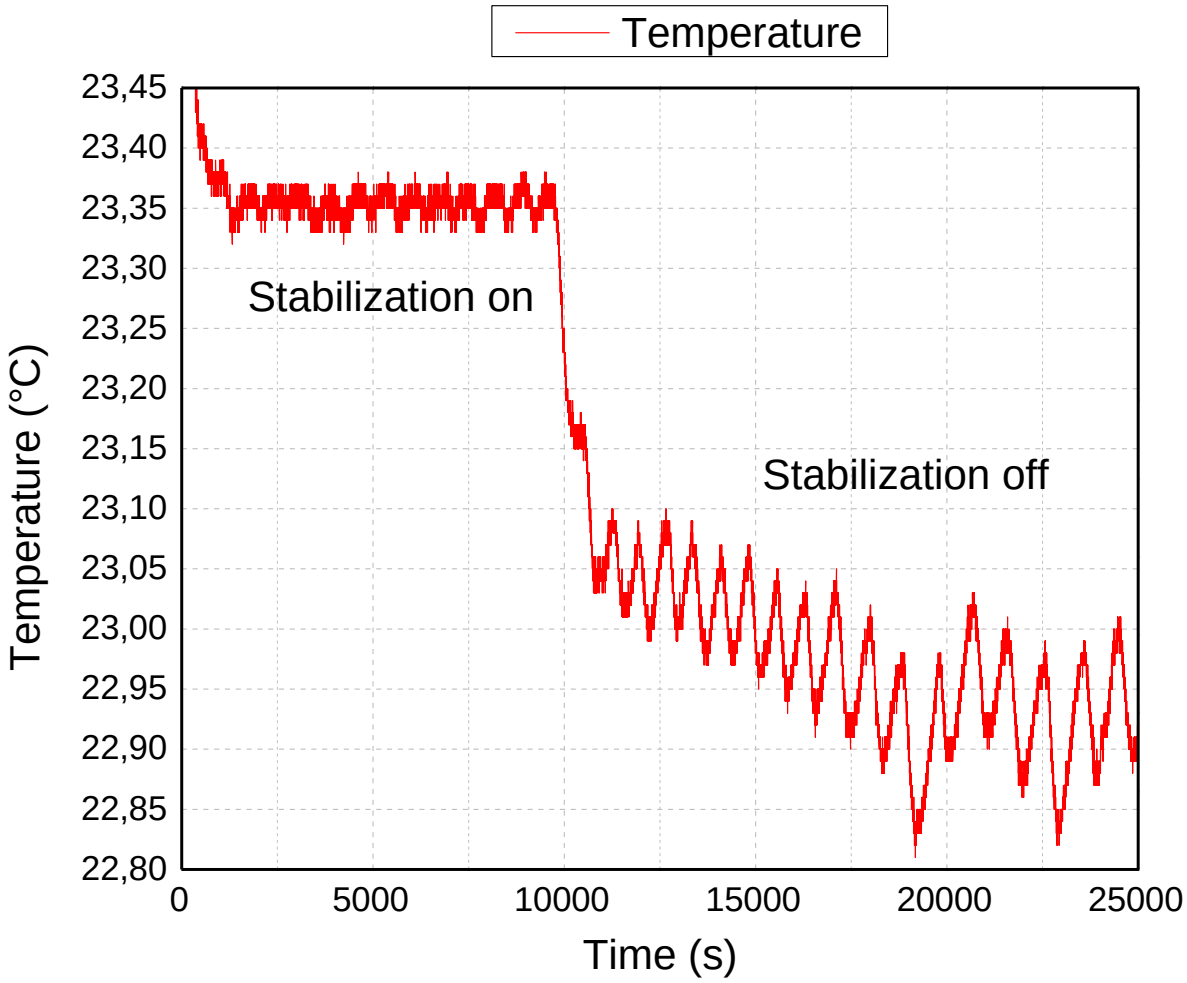

Figure 17: Temperature stabilization with the new stabilization system. The standard deviation of the temperature is ±0.01°C while the PID controller is on and ±0.08°C after it is turned off (at 10000s).

The PID starts its operation as soon as the temperature (which is controlled by the A/C) crosses the PID set point. This happens at around 500 s. For approximately 2.5 hours the temperature stays almost fixed an average temperature of 23.35°C and with a standard deviation of ±0.01°C, until the PID is turned off at around 10000s. Then the temperature starts drifting towards the A/C unit's set point until it starts oscillating around the 22.9°C value, with a standard deviation of ±0.08°C.

Comments

The new stabilization system reduced the temperature fluctuations that normally occur from the operation of the A/C, by eight times. Furthermore it kept the temperature very near the set point for a significantly long period (2.5 hours), both which are objectives in

order to improve the MOT's performance. The next step is to gather data from inside the MOT, while the stabilization system operates, in order to see whether it actually works better. This is discussed in the next chapter.

Chapter 5 The effect of the temperature stabilization on the cold atoms

In this chapter the effect of the stabilization system on the MOT's performance is discussed. Two properties we are interested in are the number of atoms in the MOT and the position of the atom cloud, both of which should not vary much in order perform BEC experiments. Specifically atom number should be sufficiently constant for condensation to occur and the cloud position should be steady for loading the atoms quickly and smoothly into the magneto-optical trap. Data was collected for both these features in order to investigate whether the stabilization system improved the MOT's stability.

Temperature fluctuation effects on the number of atoms

First we examine the possible effects of the temperature on the atom number. After the stabilization system was set up inside the BEC1 box it was turned on and stabilized the temperature. After a while it was turned off, letting the A/C unit control the temperature on its own. At the same time the number of thermal atoms inside the MOT was being monitored, as well as the temperature inside the BEC1 box. The atom number data that are presented in the below graph, were collected at the same time as temperature data of Figure 18.

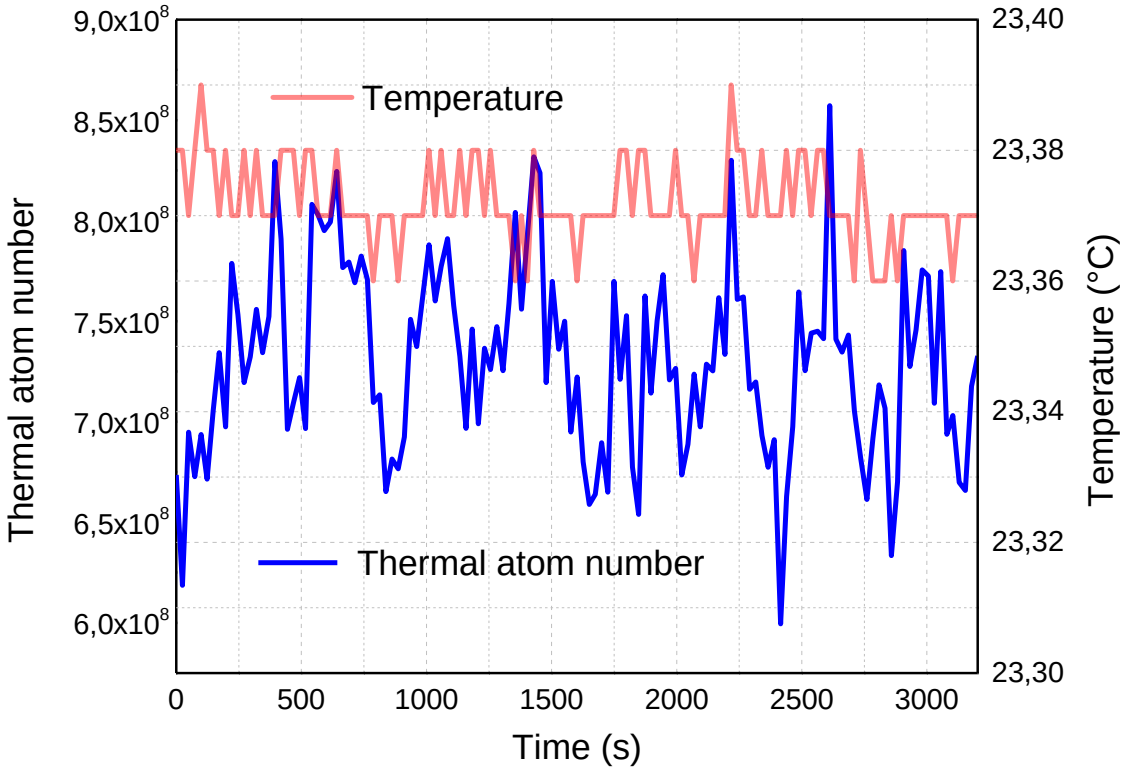

Figure 18: Number of atoms and temperature while the stabilization system is on. The standard deviation of the atom number is $\pm 4.7 \cdot 10^8$ atoms and that of the temperature is improved eight-fold to ±0.01°C.

The above figure corresponds to a portion of the time that the temperature was being stabilized, and its standard deviation was ±0.01°C. The average atom number is $7.3 \cdot 10^8$ while the standard deviation is $\pm 4.7 \cdot 10^8$ atoms.

The same procedure was carried out when the stabilization system was turned off. The atom number and the temperature were being measured simultaneously. This time the average temperature deviation was ±0.08°C. The average number of atoms was $6.7 \cdot 10^8$ and the standard deviation is $\pm 5.6 \cdot 10^8$ atoms. The temperature and atom number are shown in the figure below.

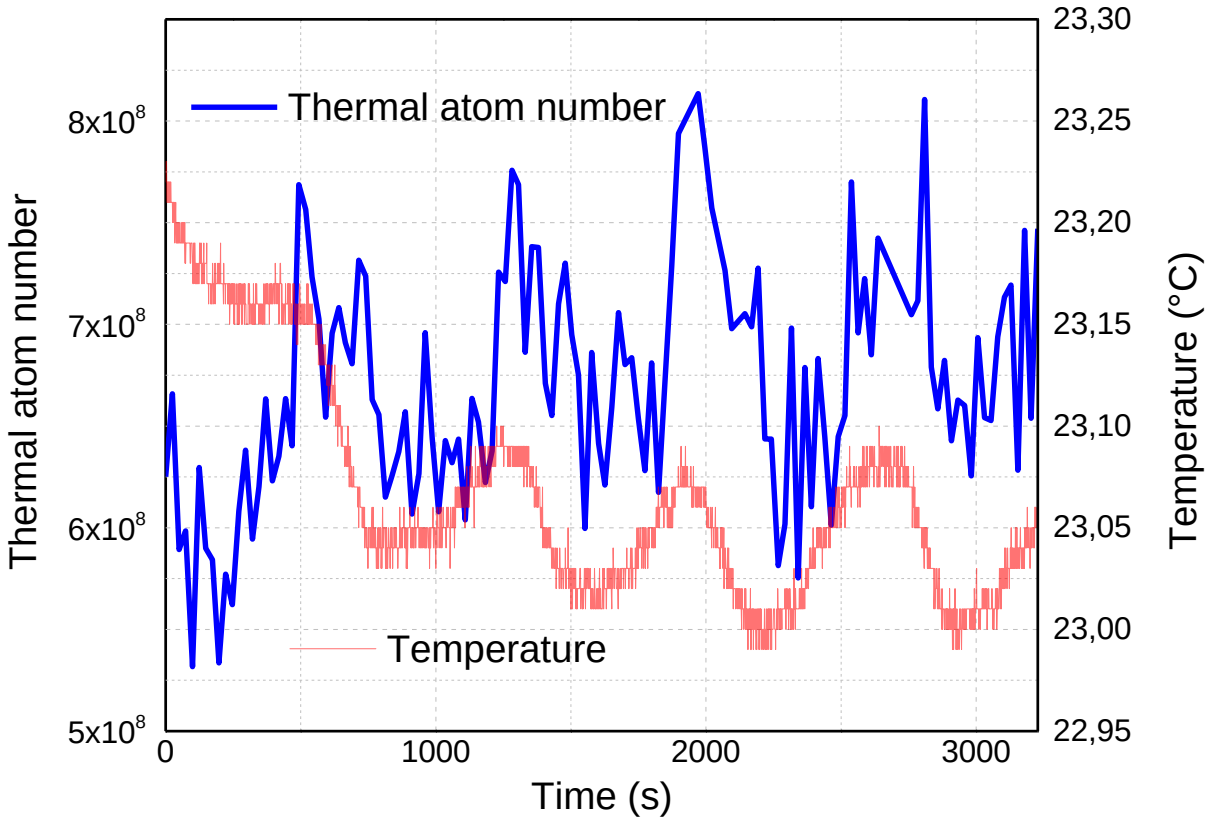

Figure 19: Number of atoms and temperature while the stabilization system is off. The standard deviation of the atom number is $\pm 5.6 \cdot 10^8$ atoms and that of the temperature is ±0.08°C.

We see that the standard deviation of the number of atoms increased by 19% when the stabilization system was turned off. To assess the correlation between variations in temperature and the number of atoms we calculate the Pearson and Spearman correlation coefficients for the whole data set of temperature and atom number. To do this we linearly interpolated the atom number data to match the size of the temperature data set. Both of these calculations were done with Origin. The calculation produced the values below.

Atom number/temperature correlation	Coefficient value
Pearson	0.34
Spearman	0.28

Table 3.1: Correlation coefficients of the number of atoms and temperature.

Comments

Even though the temperature fluctuations were reduced by a factor of eight, the atom number fluctuations were improved only marginally. It seems that the correlation is not strong between the number of atoms and the temperature variations and that the main cause of the atom number fluctuation lies elsewhere.

Temperature inside the BEC box and cloud position

After the unsuccessfully trying to mitigate the problem of fluctuating atom number in the MOT using the stabilization system, we attempted to investigate whether the stabilization system can improve the stability of the atomic cloud's vertical position. To demonstrate this, we made the MOT very sensitive to temperature changes. This was done by putting a $\frac{\lambda}{4}$ plate in front of one of the optical fibers that provides the laser light to the z direction, and another $\frac{\lambda}{4}$ plate in front of the cube in the vertical imaging axis. The A/C temperature was set to 22.1°C while the PID set point was set at 22.55°C. We first let the stabilization system stabilize the temperature, and then start looking at the position of the atom cloud. Then, after letting the experiment run for a while with the temperature stabilized, the PID controller was switched off, letting only the A/C unit control the temperature inside the BEC1 box. The results are shown in the graph below and the temperature data was collected with the Microlite-RH thermometer, which was set to measure the temperature every three seconds.

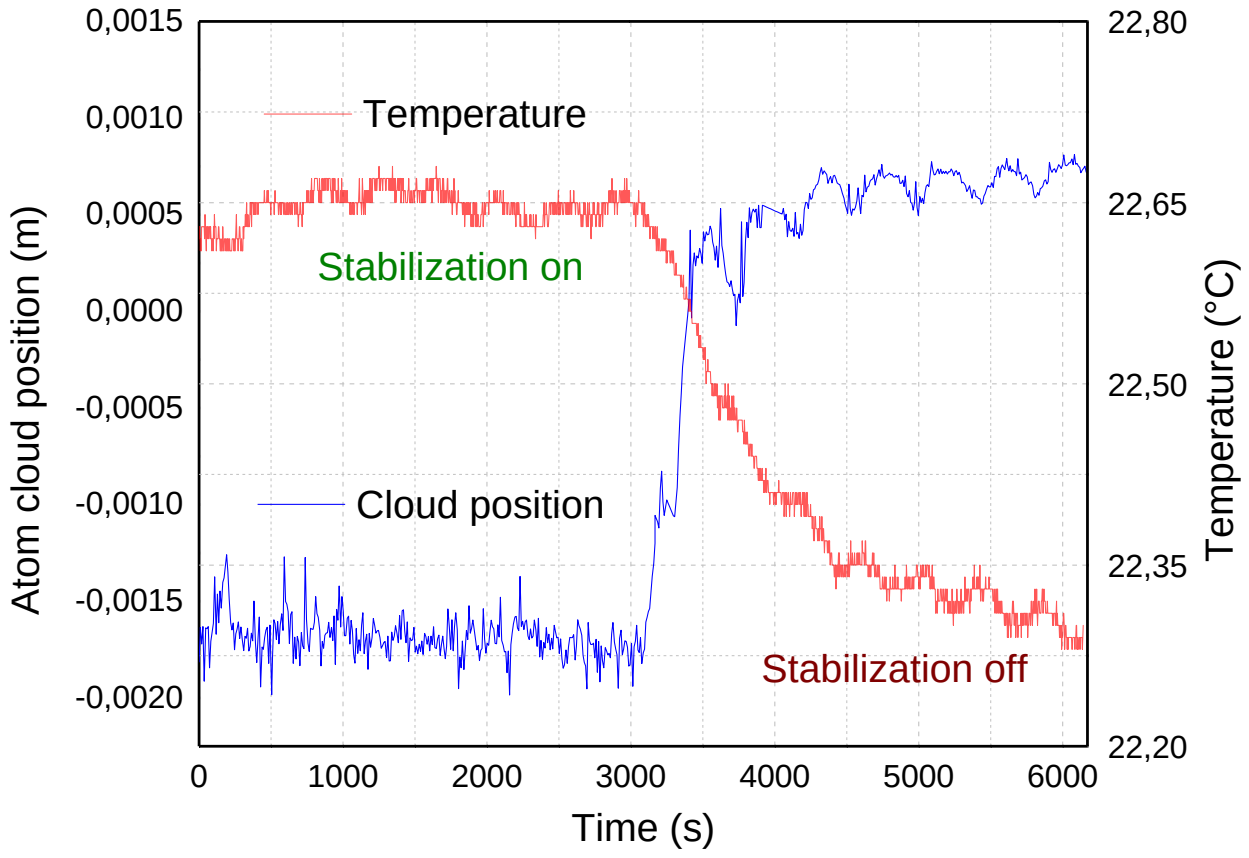

Figure 20: Cloud position (blue) and temperature inside the BEC1 box (red). In the left of the graph the stabilization system is operating with ±0.01°C fluctuations. After 3000 seconds it is turned off and the fluctuations rise at ±0.06°C. The cloud position standard deviation is ±0.00011m and ±0.00016m respectively.

From 0s to 3000s the stabilization system is operating and the average temperature is 22.65°C with a standard deviation of ±0.01°C. The average cloud position is -0.00168m with a standard deviation of ±0.00011m. As soon as the stabilization system is turned off the temperature drops immediately with ±0.06°C standard deviation, and there is a jump in the atom cloud position with an average position of 0.00059m and a standard deviation of ±0.00016m. The standard deviation increased by approximately 45% in comparison to when the stabilization system was operating, and is apparent from inspection of the graph the cloud is oscillating with a period of approximately 500s which coincides with the period of temperature oscillation, compared to before when it randomly trembles . Furthermore, the cloud position minima follow the temperature maxima after turning off the stabilization system. The same calculation of correlation coefficients was carried out for this part and are presented in the table below.

Cloud position/temperature correlation	Coefficient value
Pearson	-0.96
Spearman	-0.86

Table 3.2: Correlation coefficients of the cloud position and temperature.

Comments

We see that there is a much stronger correlation between the temperature and the cloud position. Also the correlation coefficients are negative, meaning that one increases when the other decreases and vice versa, something that was obvious from inspection of the graph. Although there are small oscillations when the stabilization system is operating the movement of the atom cloud is random. As soon as the stabilization system is turned off, the cloud starts following the oscillation of the temperature.

Chapter 6 Summary and conclusions

We demonstrated the ability to stabilize ne the temperature of the BEC experiment's surrounding environment. Our stabilization system was able to control the temperature well beyond the limits of the commercial air-conditioning unit, by utilizing a precision of PID controller and fast feedback. The stabilization system was able to reduce the temperature fluctuations up to eight times and largely reduce the fluctuation in the number and position of the ultra-cold atom clouds. The temperature was stabilized to the desired set point for a considerably very long time. Both of these improvements can be seen in Figure 17 and are important for the optimal performance of the experiment.

The ultimate goal was to improve the stability of the magneto-optical trap, the main apparatus of the experiment. The two properties of the MOT that we tried to improve were the number of atoms and the position of the atomic cloud and in terms of stability this meant that the goal was to keep the atom number as constant as possible and prevent the atom cloud from following the oscillation of the temperature. The atom number fluctuations were reduced by 19%, although the low correlation coefficient values (Table 3.1) cannot give a definite answer on whether our stabilization system was the reason for this improvement. On the other hand, the strong anti-correlation between the temperature and the cloud's position is indicating that it was in fact the stabilization system responsible for the 45% improvement of the cloud's stability in space and its more stable movement.

Bibliography

[Online] // Engineering Toolbox. - http://www.engineeringtoolbox.com/air-properties-d_156.html.

Alan V. Oppenheim Alan S. Willsky, S.Hamid Signals and Systems (2nd Edition) [Book]. - [s.l.] : Prentice-Hall International Inc., 1996.

Astrom Murray Feedback System: An introduction for scientists and engineers [Book]. - [s.l.] : Princeton University Press, 2008.

Bolpasi Vassiliki High Power Laser System for the Creation of Bose-Einstein Condensations. - 2008.

Bruce R. Kusse Erik A. Westwig Mathematical Physics, Applied Mathematics for Scientists and Engineers 2nd Edition [Book]. - [s.l.] : WILEY-VCH Verlag, 2006.

C.J. Pethick H.Smith Bose-Einstein Condensation in dilute gases [Book]. - [s.l.] : Cambridge University Press, 2008.

Dedman et. al Precision temperature controlled filtered laminar air enclosure [Journal]. - [s.l.] : IOP Publishing, 2015. - 26.

Dvorak Maschke, Vlcek The Response of Polarization Maintaining Fibers Upon Temperature Field Disturbance [Journal] // Optics and Optoelectronics. - 2014. - 2 : Vol. 12.

Geremia JM An Introduction to Control Theory: From Classical to Quantum Applications - Course Lecture Notes [Book]. - 2003.

Granino A. Korn Theresa M. Korn Mathematical Handbook for Scientists and Engineers (2nd Edition) [Book]. - [s.l.] : McGraw-Hill, 1967.

J.G. Ziegler N.B. Nichols Optimum setting for automatic controllers [Journal]. - [s.l.] : American Society of Mechanical Engineers, 1942.

John Doyle Bruce Francis, Allen Tannenbaum Feedback Control Theory [Book]. - [s.l.] : Macmillan Publishing, 1990.

John H. Matthews Russel W. Howell Complex Analysis for Mathematics and Engineering, p.429 [Book]. - Sudbury, MA : Jones and Bartlett Pub. Inc., 1999.

Joseph DiStefano Allen Stubberud, Ivan Williams Schaum's Outline of Theory & Problems of Feedback and Control Systems, Second Edition [Book]. - [s.l.] : McGraw-Hill, 1990.

Lett P.D. Optical Molasses [Journal] // Journal of the Optical Society of America. - 1989. - 11 : Vol. 6.

M. Pappa P. C. Condylis, G. O. Konstantinidis, V. Bolpasi, A. Lazoudis, O. Morizot, D. Sahagun, M. Baker, and W. von Klitzing Imaging Bose-Einstein Condensates at Ultra-Low Atom-Numbers and Time Averaged Adiabatic Potentials [Journal] // New Journal of Physics. - 2011.

Ozbay Hitay Introduction to Feedback Control Theory [Book]. - [s.l.] : CRC Press, 1999.

Schetzen Martin Linear TIme-Invariant Systems [Book]. - [s.l.] : IEEE Press, 2003.

tdk.eu [Online]. - TDK. - http://en.tdk.eu/inf/50/db/ntc_13/NTC_SMD_Automotive_series_0402.pdf.

Willis M.J. Proportional-Integral-Derivative Control [Book]. - 1999.

Wilson Li Dessau Optimizing the Performance of Optical Mounting Systems [Journal] // Optics & Photonics News. - 2005.

Zhang Feng Temperature and strain sensitivity measurements of high-birefringent polarization-maintaining fibers // Physics an Computer Science Publications. - [s.l.] : Wilfrid Laurier University, 1993.